Starvation of the bacteria *Vibrio atlanticus* promotes lightning group-attacks on the dinoflagellate *Alexandrium pacificum*

Jean Luc Rolland[1, 2†*], Estelle Masseret[3], Mohamed Laabir[3], Guillaume Tetreau[4], Benjamin Gourbal[4], Anne Thebault[5], Eric Abadie[6], Alice Rodrigues-Stien[7,8], Carole Veckerlé[7,8], Elodie Servanne-Meunier[1], Delphine Destoumieux-Garzón[1], Arnaud Lagorce[4,9] , Raphaël Lami[7,9].

Affiliations

[1]IHPE, Univ. Montpellier, CNRS, IFREMER, Université de Perpignan Via Domitia, Montpellier, France.

[2]MARBEC, Univ. Montpellier, IRD, IFREMER, CNRS, Sète, France.

[3]MARBEC, Univ. Montpellier, IRD, IFREMER, CNRS, Montpellier, France.

[4]IHPE, Univ Montpellier, CNRS, IFREMER, Université de Perpignan Via Domitia, Perpignan, France

[5]Agence nationale de sécurité sanitaire de l'alimentation, de l'environnement et du travail (ANSES), ANSES-DER 27-31, avenue du Général Leclerc, 94701 Maison-Alfort, France

[6]IFREMER, 9 rue Jean Bertho, 97822, Le port, la Reunion, France

[7]Sorbonne Université, CNRS, LBBM USR3579, Observatoire Océanologique de Banyuls sur Mer, Avenue Pierre Fabre, 66650 Banyuls-sur-Mer, France.

[8]Sorbonne Université, CNRS, Bio2MAR, Observatoire Océanologique de Banyuls sur Mer, Avenue Pierre Fabre, 66650 Banyuls-sur-Mer, France.

[9]These authors contributed equally

[†]Current address

*Corresponding author: Jean Luc.Rolland

Email: Jean.Luc.Rolland@ifremer.fr

ABSTRACT

Algae serve as a source of nutrients for bacteria in the marine environment. The interactions between algae and bacteria at the phycosphere interface are known to include mutualism, commensalism, competition or antagonism. Here, based on *in situ* observation and on an *in vitro* interaction study, we report on a novel form of starvation-induced hunting that the cells of selected *Vibrio* species exert on the dinoflagellate species. Results showed that *Vibrio atlanticus* was able to coordinate lightning group attacks then kill the dinoflagellate *Alexandrium pacificum* ACT03. Briefly, the observed coordinated mechanism of algal-killing consists of first, the 'immobilization stage' involving the secretion of algicidal metabolites that disrupt the flagella of the prey. The 'attack stage' resembles the 'wolf-pack attack' strategy, during which *Vibrios* surrounds algal cells at high density for a brief period without invading them. Finally, the 'killing stage' induces the lysis and degradation of the dinoflagellates.

By using a combination of biochemical, proteomic, genetic and fluorescence microscopy approaches, we showed that this relationship is not related to the decomposition of algal organic matter, *Vibrio* quorum sensing pathways, to the toxicity of the algae or to the pathogenicity of the bacterium but is conditioned by nutrient stress, iron availability and link to the iron-vibrioferrin transport system of *V. atlanticus*. This is the first evidence of a new mechanism that could be involved in regulating Alexandrium spp. blooms and giving Vibrio a competitive advantage in obtaining nutrients from the environment.

KEYWORDS

Interaction; Bacterium; Alga; Predation; Environment; Iron related predation

INTRODUCTION

Harmful algal blooms (HABs) have experienced an increase in their occurrence, intensity, and geographical distribution on a global scale, resulting in adverse environmental, health, and socioeconomic impacts (Marampouti et al., 2021). HABs have a considerable impact on human health as a result of direct exposure to volatile toxins or by toxic seafood consumption (Burkholder et al., 2018). From an ecological point of view, the expansion of HABs can result in the erosion of biodiversity, because they cause massive mortality of marine species and they are generally monospecific in nature (Chai et al., 2020). In coastal areas, understanding the biological interactions that control toxic algal blooms is therefore a major ecological challenge. Among HABs, a number of *Alexandrium* species have been placed on the list of invasive Mediterranean species. Among them, *Alexandrium pacificum* is a flagellated eukaryotic unicellular organism that form with *Alexandrium tamarense* and *Alexandrium fundyense* the "Alexandrium tamarense" complex (Hadjadji et al., 2020). Since 1998, *A. pacificum* (former *A. catenella*) was monitored by Rephy survey in the Thau lagoon (French Mediterranean) because it produces paralytic shellfish toxins (PSTs) resulting of paralytic shellfish poisoning (PSP) syndrome.

Laania (Laanaia et al., 2013) showed that in Thau lagoon, a water temperature around 20°C for several days and organic and inorganic nutrients in sufficient concentrations are parameters favoring the developemnt of *A. pacificum*, whose massive blooms occur in autumn.

Algal blooms are seasonal events resulting in a rapid increase in the concentration of a species of algae in an aquatic environment. Depending on the phytoplankton species, the tolerance range of physicochemical parameters is different and influences the time of appearance of blooms (Leblad et al., 2020).

Interestingly, although the collapse of phytoplankton blooms has been previously attributed to viruses (Pal et al., 2020), some ecological studies have suggested an important role of algicidal bacteria (Su et al., 2007; Wang et al., 2010), such as some Vibrio *spp*. (Li et al., 2014; Wang et al., 2020).

Vibrio (class γ-proteobacteria) are common microorganisms in marine systems worldwide (Baker-Austin et al., 2017; Mavian et al., 2020), where they are important components of the food chain, particularly in

biodegradation, nutrient regeneration and biogeochemical cycles (Oberbeckmann et al., 2012). Vibrio is one of the most studied bacterial taxa due to their ubiquity in coastal marine systems and their capacity to cause infections in humans and animals, leading sometimes to epizootic or zoonotic epidemics (LeRoux et al., 2015; Mavian et al., 2020). *Vibrio* are extremely adaptable to their environment (Johnson, 2013). The main factors influencing their occurrence and distribution in water are temperature, salinity, nutrient availability (Wang et al., 2020), multiple strategies such as biofilm formation on biotic and abiotic surfaces (Espinoza-Vergara et al., 2020), or interactions with a multitude of other organisms such as eukaryotic predators (Drebes Dörr and Blokesch, 2020) or plankton (Lopez-Joven et al., 2018) are used by *Vibrio* in the environment. There is also evidence that global climate change has increased *Vibrio*-associated illnesses affecting humans and animals (Brumfield et al., 2021; Muhling et al., 2017). However, the drivers and dynamics of *Vibrio* survival and propagation in the marine environment are not yet fully understood.

A substantial number of research articles have highlighted the potential of γ-proteobacteria to exert algicidal activity against dinoflagellates, supporting the hypothesis that γ-proteobacteria such as *Vibrio* play a role in the control of algae blooms *in situ* (Coyne et al., 2022). However, the mechanisms behind *Vibrio*-driven algal lysis in the environment remain to be elucidated. Particularly, it is unclear how in the water column, algicidal compounds secreted by bacteria can concentrate around the algae to exert their lytic effect.

Based on observations from the natural environment showing a potent relationship between *Vibrio* and *Alexandrium* algae bloom events, this study aim to determine *in vitro,* the main factors implicated in this relationship. Using a combination of biochemical, proteomic, genetic, and fluorescence microscopy approaches, we explored the role of algal toxicity, bacterial pathogenicity and the quorum sensing pathway on this relationship and showed the important role of nutrient stress and the iron uptake pathway in this unique Vibrio/Alexandrium predator/prey interaction.

METHODS

Quantification of *Alexandrium* algae and *Vibrio* bacteria in the environment.

Seawater samples were collected in the Thau Lagoon (southern France, a shallow Mediterranean ecosystem open to the sea (Abadie et al., n.d.), during spring and autumn 2015. Briefly, samples were collected from the subsurface (-50 cm) near an oyster table at a phytoplankton surveillance site (part of the REPHY network, N 43°26.058' and E 003°39.878'). Once a week during spring and autumn 2015, during field sampling campaigns, 20 L of water was filtered on board through a 180 µm pore-size nylon membrane. At the laboratory, according to Lopez-Joven et al. (Lopez-Joven et al., 2018) seawater was fractionated into two size classes as follows: 2 L of the above filtrate was filtered through a 0.8 µm pore-size polycarbonate Whatman Nuclepore membrane to obtain organisms in the 0.8–180 µm range corresponding to plankton-associated *Vibrio* and living *Alexandrium* forms. Then, the filtrate from the 0.8 µm membrane was filtered again through a 0.2 µm pore-size polycarbonate Whatman Nuclepore membrane until the membrane was saturated. *Alexandrium* cells, ranging from 25 to 40 µm, belong to the microphytoplankton and are therefore retained in the 0.8–180 µm fraction. Any *Vibrio* cells potentially associated with or attached to *Alexandrium* cells will also be retained in this fraction. *Vibrio* cells are approximately 0.5-0.8 µm-thick. The fraction between 0.2 and 0.8 µm therefore includes the free-living *Vibrio*. The bacterial population collected on 0.8-µm-pore-size filters was designated the particle-associated community, and the population on 0.2-µm-pore-size filters was designated as the free-living community. Membranes (in triplicate) were then conserved in 500 µL of 100% EtOH at -20°C. Environmental DNA (eDNA) was extracted from the MF Millipore membrane using the Macherey-Nagel NucleoSpin Tissue Kit and resuspended in 100 µL of water. The samples were then stored at -20°C after eDNA quantity and purity were assessed using a NanoDrop system (NanoDrop Technologies, Wilmington, DE, USA). PCR amplification reactions were done on a Roche LightCycler 480 Real-Time

thermocycler (qPHD platform, University of Montpellier, France).using specific primer pairs (Table 3). Typically, the reactions contained 1 µL of template DNA (the DNA concentration for all samples varied from 1 to 40 µg mL^{-1}), 0.5 µL of each primer (3.33 µM) and 4 µL of reaction mixture (SYBR Green Master Mix) in a total volume of 6 µL. The reaction parameters were as follows: 5 minutes at 95°C (initial denaturation) and 40 cycles of 10 s at 95°C (denaturation), 10 s at the corresponding hybridization temperature (Table 3) and 10 s at 72°C (elongation). Melting curve profiles were generated by increasing the temperature from 65°C to 95°C at 0.5°C s^{-1}. Amplification products were analysed using LightCycler software (Roche Diagnostics). *Vibrio spp*. and *A. pacificum* and *A. tamarense* were quantified by constructing calibration curves based on DNA from the *V. atlanticus* LGP32 reference strain (former *V. tasmaniensis* LGP32) and from the *A. pacificum* reference strain (ACT03: *A. catenella* strain isolated form Thau in 2003) and the *A. tamarense* reference strain (ATT07: *A. tamarense* isolated from Thau in 2007) (not shown).

Strains and growth conditions.

Vibrio strains. Wild-type and isogenic mutants of *Vibrio atlanticus* LGP32 (Table 1) were used in this study. Deletion-mutants included Δ*luxR*, Δ*luxP*, Δ*luxM* and Δ*pvuB* isogenic strains. The Δ*pvuB* mutant was constructed here by allelic exchange as described previously by Le Roux (Le Roux et al., 2007). We also used *V. atlanticus* LGP32 carrying the pSW3654T-GFP plasmid (Le Roux et al., 2007), hereafter referred to as *V. atlanticus* LGP32-GFP. Bacterial strains were grown at 22 ± 1°C in Zobell medium (0, 38 µM iron (III)). When needed, 25 µg mL^{-1} chloramphenicol (Cm) was added to cultures of *V. atlanticus* LGP32-GFP (Le Roux et al., 2007). Oligonucleotides used for RNA expression analysis are specified in table 3.

Phytoplancton strains. Non-axenic phytoplankton species (Table 2) were grown in batch culture in enriched natural sea water (ENSW, 6,55 µM iron (III)) with a salinity of 36 practical salinity units (PSU) at 22 ± 1°C under cool white fluorescent illumination (100 µmol photons m^{-2} s^{-1}) and a 12 h:12 h

144 light:dark cycle (Harrison et al., 1980). The algae were used for experiments in their exponential growth
145 phase.

146 **Co-culture assay**

147 For each tested phytoplankton species, 2.10^4 cells harvested in their exponential growth phase were placed
148 in 20 mL of ENSW medium in a 50 mL suspension culture flask (Cellstar® PS, Greiner bio-one). After
149 incubation for 24 h at 22 ± 1°C under cool white fluorescent illumination, 40 µL of *Vibrio* strains grown
150 for 12, 36, 60 and 156 h in Zobell medium or in Zobell medium supplemented with $Fecl_3$ (6 µM iron (III))
151 or with H_3BO_3 (0.47 mM) or the corresponding culture supernatant were added to the algal culture. After
152 incubation at 22 ± 1°C under cool white fluorescent lights, living, non-swimming, group-attacked and
153 lysed phytoplankton cells were counted in a sedimentation chamber under an inverted microscope. The
154 number of lysed cells corresponded to algae showing disrupted membranes. Non-swimming algae were
155 not counted as lysed cells. For *Vibrio* analysis, 100 µL of a 1:10 serial dilution mixture in ENSW (from
156 10^{-2} to 10^{-10}) was plated on *Vibrio* Selective TCBS (thiosulfate-citrate-bile salts-sucrose) agar (in
157 triplicate). After incubation for 24 h at 22 ± 1°C, the number of living *Vibrio* cells was determined by
158 counting colony-forming units (CFUs). Data are the means of three independent experiments.
159

160 **Microscope observations**

161 The dynamic of the interaction between *A. pacificum* ACT03 and *V. atlanticus* LGP32, which is an oyster
162 pathogen isolated from the French Atlantic coast (Gay et al., 2004) and present in the Thau Lagoon, south
163 of France (Lopez-Joven et al., 2018)) was surveyed. As the algal strain used in the study is not axenic,
164 means that additional bacteria, other than the *V. atlanticus* LGP32, are present in the experiments.
165 To elucidate the interaction without thoroughly accounting for the non-axenic cells, interaction was
166 observed under a Zeiss Axio upright fluorescence microscope equipped with an AxioCamMRm 2 digital
167 microscope camera using *V. atlanticus* LGP32 tagged with green fluorescent protein (GFP). Lasers were

used at excitation wavelength (λex) 488 nm for GFP (emission wavelengths (λem): 505–530 nm) and λex 532 nm for plankton chloroplasts (λem 560–630 nm). Images were taken sequentially to avoid cross-contamination between fluorochromes. Sequences of images were merged during the *Vibrio-Alexandrium* interaction using ZEN 2012 (blue edition) software. Interaction events between *Vibrio* strains and phytoplankton strains were also observed under a Leica TCS SPE confocal laser scanning system connected to a Leica DM 2500 upright microscope camera (Montpellier RIO Imaging Platform, University of Montpellier, France).

Comparative proteomic analysis

Vibrio sampling and protein extraction. V. atlanticus LGP32 was grown for 60 h at 22°C in artificial seawater (high nutrient stress, cond. 1) or 12 h at 22°C in Zobell media (low nutrient stress, cond. 2). After 10 min centrifugation at 8000 rpm, crude protein extracts of *V. atlanticus* LGP32 in each culture condition (triplicates) were obtained by sonication on ice at 20% amplitude for 20 s in 200 µL of ice-cold denaturing buffer (7 M urea, 2 M thiourea, 4% CHAPS in 30 mM Tris-HCl, pH 8.5) and clarified by centrifugation at 2000 x *g*, 15 min, 4°C. The protein concentration of the supernatant was estimated using the 2D Quant Kit (Cytiva™, MERCK) and samples were stored at -80°C until use.

Bi-dimensional gel electrophoresis (2D gel). Proteins extracts were individually analysed on 2D gel electrophoresis (6 gels per condition each corresponding to different biological replicates). To do so, 100 µg of proteins from each extract was added to rehydration buffer (7 M urea, 2 M thiourea, 4% CHAPS, 65 mM DTT) for a total volume of 350 µL. They were then individually loaded onto 17 cm isoelectric focusing strips (Bio-Rad) with a stabilized non-linear pH ranging from 3 to 10. Due to the high complexity of the protein profile in the acidic part (left) of the gel pH 3–10 (Fig. S3), we conducted additional 'close-up' analyses in gels using 17 cm isoelectric focusing strips (Bio-Rad) with a narrower, stabilized pH gradient ranging from 4 to 7. Strips were rehydrated passively for 5 h at 22°C, followed by

192 active rehydration for 14 h under a 50 V current at 22°C (to help large proteins enter the strips).
193 Thereafter, isoelectrofocusing was carried out using the following programme: 50 V for 1 h, 250 V for 1
194 h, 8000 V for 1 h and a final step at 8000 V for a total of 140 000 V.h with a slow ramping voltage
195 (quadratic increasing voltage) at each step. Focused proteins were reduced by incubating the strip twice in
196 equilibration buffer (1.5 M Tris, 6 M urea, 2% SDS, 30% glycerol; bromophenol blue, pH 8.8) containing
197 DTT (130 mM) at 55°C. Then, they were alkylated by incubation with equilibration buffer containing
198 iodoacetamide (135 mM) on a rocking agitator (400 rpm) at room temperature protected from light.
199 Proteins were also separated according to their molecular weight (second dimension) on 12%
200 acrylamide/0.32% piperazine diacrylamide gels run at 25 mA per gel for 30 min followed by 75 mA per
201 gel for 8 h using a Protean II XL system (Bio-Rad). Gels were stained using an MS-compatible silver
202 staining protocol and scanned using a ChemiDoc MP Imaging System (Bio-Rad) associated with Image
203 Lab software version 4.0.1 (Bio-Rad).
204
205 *Comparative bioinformatics analysis of 2D gels.* Twelve gels (six per condition) were selected for
206 comparative analysis on PD-Quest v. 7.4.0 (Bio-Rad) to identify changes in protein abundance between
207 the proteomic profiles of *V. atlanticus* LGP32 cultured in contrasting nutrient conditions (ENSW/Zobell).
208 Spots whose mean intensity across six replicates per strain was two times higher or lower than those from
209 the other strain, with a $P < 0.01$ (Mann-Whitney U-test), were considered significantly different in terms of
210 abundance between the two conditions (quantitative difference). Differentially represented spots were then
211 excised from the gels, destained, trypsin-digested and the obtained peptides were identified by tandem
212 mass spectrometry (MS-MS) using the PISSARO platform facility (University of Rouen, France). To
213 identify protein(s) present in each spot, the obtained peptides were compared with *V. atlanticus* LGP32
214 reference genome *(https://vibrio.biocyc.org/)*. The genes whose peptides matched strongly were retrieved
215 and used for an BLASTx query against non-redundant databases to determine the protein identity of the
216 best match. A gene was considered as strongly matched when at least two peptides matched the sequence

with a coverage of> 6%. Their theoretical isoelectric point (pI) and molecular weights were also calculated using the Expasy server (https://www.expasy.org/) to compare them with the location of the spot on the gel. Altogether, these complementary analyses made it possible to characterize the protein identity of each spot with confidence.

Gene expression analysis

Vibrio sampling and RNA extraction. V. atlanticus LGP32 was grown in Zobell media for 36 h and 60 h at 22°C (decline phase of growth, nutrient stress) or for 12 h at 22°C (exponential grow phase, poor nutrient stress). Total RNA was isolated from *V. atlanticus* LGP32 using the standard TRIzol method (Invitrogen Life Technologies SAS, Saint-Aubin, France) and then treated with DNase (Invitrogen) to eliminate genomic DNA contamination. After sodium acetate precipitation, the quantity and quality of the total RNA were determined using a NanoDrop spectrophotometer and agarose gel electrophoresis. Following heat denaturing (70°C for 5 minutes), reverse transcription was performed using 1 µg of RNA prepared with 50 ng μL^{-1} oligo-(dT) 12–18 mer in a 20-µL reaction containing 1 mM dNTPs, 1 unit μL^{-1} RNAseOUT and 200 units μL^{-1} Moloney murine leukaemia virus reverse transcriptase (M-MLV RT) in reverse transcriptase buffer, according to the manufacturer's instructions (Invitrogen Life Technologies SAS, Saint-Aubin, France).

PCR amplification. Amplification reactions were analysed using a Roche LightCycler 480 Real-Time thermocycler (Bio-Environnement platform, University of Perpignan, France). In this study, several PCR primer pairs were designed using Primer3 software (optimal primer size: 20 bases; Tm: 60°C; primer GC%: 50; 2GC clamp and product size range: 150–200 bp) and calibrated with *V. atlanticus* LGP32 genomic DNA (Table 1). To determine the qPCR efficiency of each primer pair used, standard curves were generated using seven serial dilutions of genomic DNA (10^{-2}, 10^{-3}, 10^{-4}, 10^{-5}, 10^{-5}, 10^{-7} and 10^{-8}) (not

241 shown); the qPCR efficiencies of the tested genes varied between 1.85 and 2.08 (Table 3). For gene
242 expression, reverse transcription was performed with 1 µg of total RNA using random hexamers and
243 SuperScript IV reverse transcriptase (Invitrogen). The total qPCR reaction volume was 10 µL and
244 consisted of 5 µL of cDNA (diluted 1:5), 2.5 µL of SensiFAST SYBR No-ROX Mix (Bioline) and 100
245 nM or 300 nM PCR primer pair (Table 3). The reaction parameters were as follows: 2 min at 95°C (initial
246 denaturation) and 40 cycles of 5 s at 95°C (denaturation), 10 s at 59°C (annealing) and 20 s at 72°C
247 (elongation). The specificity of each PCR was checked by measuring fluorescent signals during melting
248 curve analysis (PCR product heated from 65°C to 95°C continuously and slowly at 0.1°C s^{-1}). Relative
249 expression was calculated by normalization to the expression of two constitutively expressed
250 housekeeping genes, namely, 6PKF (VS_2913) and CcmC (VS_0852), using the delta-delta threshold
251 cycle (ΔΔCt) method(Pfaffl, 2001).

252

253 **Detection of quorum-sensing signalling molecules**.
254 *Vibrio culture.* To detect the QS molecules (AI-2, AI-1 and CAI-1) *V. atlanticus* LGP32 was grown
255 in Zobell media for 12 h (exponential growth phase, control) and 60 h (decline phase of growth, nutrient
256 stress).
257 *AI-2 analysis.* Bioluminescence assay using the QS bioluminescent of *Vibrio campbellii* MM32
258 (*luxN*::Cm, *luxS*::Tn5Kan) was used to detect AI-2 molecules in culture supernatants. Briefly, *Vibrio*
259 cultures were centrifuged at 17,000 x *g* for 10 min, and the resulting supernatants were filtered on 0.22
260 µm. Then 20 µL of the filtrates were mixed with 180 µL of *V. campbellii* MM32 diluted 1:5000 then
261 incubated at 30°C and 100 rpm. Luminescence and cell density (OD620) were collected in triplicate and
262 analysed according to Tourneroche et al.(Tourneroche et al., 2019).
263

AI-1 and CAI-1 extraction and LC-MS analysis. Chemical analyses were conducted with a Q Exactive Focus Orbitrap System coupled to an Ultimate 3000™ ultrahigh-performance liquid chromatography (UHPLC) system (Thermo Fisher Scientific) according to Rodrigues et al. (Rodrigues et al., 2022). Briefly, ethyl acetate (2 mL) was added into each culture (2 mL). This mixture was shaken overnight at room temperature (150 rpm). The two phases were then separated and the aqueous phase was extracted once again. The two obtained organic phases were pooled and the solvent was evaporated under vacuum. The crude extracts were dissolved in 500 µL LC-MS grade methanol for analysis. All experiments were conducted in triplicate. Analyses of extracts and standards (3 µL injected) were performed in electrospray positive ionization mode in the 50–750 m/z range in centroid mode. The parameters were as follows: spray voltage: 3 kV; sheath flow rate: 75; aux gas pressure: 20; capillary temperature: 350°C; heater temperature: 430°C. The analysis was conducted in Full MS data-dependent MS2 mode (Discovery mode). Resolution was set to 70,000 in Full MS mode, and the AGC (automatic gain control) target was set to $1x10^6$. In MS2, resolution was 17,500, AGC target was set to $2x10^5$, isolation window was 0.4 m/z, and normalized collision energy was stepped to 15, 30 and 40 eV. The UHPLC column was a Phenomenex Luna Omega Polar C18 1.6 µm, 150 x 2.1 mm. The column temperature was set to 42°C, and the flow rate was 0.4 mL min^{-1}. The solvent system was a mixture of water (A) with increasing proportions of acetonitrile (B), with both solvents modified with 0.1% formic acid. The gradient was as follows: 1% B 3 min before injection, then from 1 to 15 min, a gradient increase of B up to 100% (curve 5), followed by 100% B for 5 min. The flow was injected into the mass spectrometer starting immediately after injection. All data were acquired and processed using FreeStyle 1.5 software (Thermo Fisher Scientific).

Chemicals and solvents. N-acyl-homoserine lactones (AHL) were obtained from Cayman Chemical (Ann Arbor, MI, USA). Stock solutions were obtained by dissolving standards in methanol or dichloromethane (C18-AHL) at a concentration of 1 mg mL^{-1} and stored at -80°C. Standard solutions for UHPLC- high-

289 resolution tandem mass spectrometry (HRMS) analyses were prepared by diluting each individual
290 standard solution with methanol in order to obtain a concentration range from 2000 to 20 ng mL^{-1}. LC-MS
291 grade methanol, acetonitrile and formic acid were purchased from Biosolve (Biosolve Chimie, Dieuze,
292 France), analytical-grade ethyl acetate was obtained from Sigma-Aldrich. Pure water was obtained from
293 Elga Purelab Flex System (Veolia LabWater STI, Antony, France).

294

295 **Nature of lytic compounds secreted by *V. atlanticus* LGP32**.
296 To determine the nature of the lytic compounds secreted, *V. atlanticus* LGP32 grown for 60 h in Zobell
297 media at 22 °C was filtered through a 10 kDa membrane (Amicon® Ultra-4 filter unit). The eluate
298 containing molecules with MW below 10 KDa was then incubated in a water bath at 100°C for 30 min.
299 Boiled filtrates (0.1 mL) were subsequently used to inoculate *A. pacificum* (ACT03 strain) cultures, then
300 lytic activity was observed under the Leica TCS SPE confocal laser scanning system. Zobell media with
301 the same treatment was used as control.

302

303 **Statistical analysis.***Environmental data*. Statistical analyses were performed using R 3.6.3 software. The
304 relationship between *Alexandrium* and *Vibrio* was explored separately in spring and autumn. We used a
305 generalized linear model specifying a Gaussian family. For spring, the dataset for salinity and temperature
306 was complete (14 periods of observation). One influential period was detected and removed from the
307 dataset whenever no dead *Alexandrium* cells were observed. The effects of explanatory variables such as
308 log10 (Vibrio+1), salinity and temperature were centred, reduced and tested as fixed effects with a linear
309 relationship. Model selection was performed using the Akaike information criterion corrected for small
310 sample size (AIC_c). Models were considered different whenever the difference between their AIC_c value
311 and the lowest AIC_c value (ΔAIC_c) was lower than 2 (Burnham and Anderson, 2002). *Alexandrium*

distribution and model residuals were checked for normal distribution assumptions (QQ plot and Shapiro-Wilk test). For autumn, the dataset was complete for 10 periods of observation. Salinity and temperature were missing for three periods. We explored the relationship between *Alexandrium* and *Vibrio* alone using the method detailed above for spring.

In vitro data. Statistical analyses were performed using one-way ANOVA (analysed by pair) followed by Tukey's test (Statistica 10.0 software, StatSoft, Maison-Alfort, France). *P <0.05, **P <0.01, ***P <0.001

RESULTS

Concomitant occurrence of *A. pacificum* ACT03, *A. tamarense* ATT07 and free-living *Vibrio spp.* in the Thau lagoon. In the spring and autumn of 2015, in the Thau Lagoon (Fig. 1A), we detected *Alexandrium* algae (*A. pacificum* ACT03 *and A. tamarense* ATT07, both alive and in degraded cell forms) and free-living *Vibrio*, but no plankton-associated *Vibrio* were observed (Fig. 1B, Data S1). Using model selection based on AICc, we found no significant relationship between *Alexandrium* (*A. pacificum* ACT03*, A. tamarense*) and *Vibrio Spp.* abundances in autumn. This result is consistent with the difficulty that *Vibrio* has in growing at temperatures below 20°C and with the complex interacting factors driving bloom dynamics (Laanaia et al., 2013). Interestingly, in spring 2015, the mean densities of *Alexandrium* and of free-living *Vibrio* were positively correlated. The lowest AICc was obtained with the model explaining degraded form of *Alexandrium* density based on the free *Vibrio* density (Fig. 1C). Given that, this model is not so different from the model with only the intercept, but better than any other linear combination with other potentially interfering drivers, such as temperature and salinity (Fig. 1D), we searched for evidence of a relationship between *Vibrio* and *Alexandrium* by studying their interaction *in vitro*.

335 ***Vibrio atlanticus* LGP32 feeds on *Alexandrium pacificum* ACT03**.

336 To investigate whether *Alexandrium* interacts with *Vibrio*, we incubated in Enriched Natural SeaWater
337 (ENSW) *A. pacificum* ACT03 with *V. atlanticus* LGP32 previously grown for 12 hours in Zobell media.
338 In interaction with *V. atlanticus* LGP32, *A. pacificum* ACT03 cell abundance decreased significantly from
339 2.10 x 10^4 cells mL^{-1} to 1.07 x 10^4 cells mL^{-1} after 48 h (Fig. 2A), while the *V. atlanticus* LGP32
340 concentration grew significantly after 26 h of interaction, reaching a maximum peak density of 7.67 x 10^7
341 CFU mL^{-1} at 34 h (Fig. 2B). In the control experiment where *A. pacificum* ACT03 was cultured alone in
342 ENSW, the algal concentration remained stable over time (Fig. 2A) and no bacteria were on the
343 corresponding TCBS plates (*Vibrio* selective medium). In the control where *V. atlanticus* LGP32 was
344 cultured alone in ENSW, the concentration of the bacteria tended to increase during the first 24 h (from
345 2.0 x 10^5 to 7.0 x 10^5 CFU mL^{-1}) and then decreased at 48h, below the initial starting concentration (Fig.
346 2B). These results show that the interaction between *V. atlanticus* LGP32 and *A. pacificum* ACT03 leads
347 to a decline in the algal population and promotes the growth of *V. atlanticus* LGP32. This suggests that *V.*
348 *atlanticus* LGP32 is able to feed on *A. pacificum* ACT03.

349 ***V. atlanticus* LGP32 performs group-attacks on *A. pacificum* ACT03**.

350 Epifluorescence microscopy observation of GFP-labelled *V. atlanticus* LGP32 (previously grow in Zobell
351 medium) in interaction showed that *A. pacificum* ACT03 cells that had lost their motility were attacked
352 individually by groups of *V. atlanticus* LGP32 before being lysed (Movie 1). Attacks were extremely
353 rapid, with empty thecae (algal envelopes) observed in the medium after less than 60 s (Movie 2). During
354 the attack, *V. atlanticus* LGP32 did not invade the algal cell but remained clustered on the cell surface
355 (Fig. 3A2).

356 **Group attack of *A. pacificum* ACT03 is activated by *V. atlanticus* LGP32 starvation.**

357 In 2002, Martin hypothesized that nutritional stress induces bacteria to lyse algae (Martin, 2002). To test
358 this hypothesis, we monitored *V. atlanticus* LGP32 behaviour in response to starvation (Fig. 3). We

observed that *V. atlanticus* LGP32 in exponentially growth phase (12 h of culture in Zobell medium) did not interact with *A. pacificum* ACT03 cells for the first hour of contact (Fig. 3A, B, C). In contrast, *V. atlanticus* LGP32 in the decline phase (36 h of culture in Zobell medium) induced a significant decrease in the number of motile algae cells by 8.9% after 15 min and by 43.3% after 60 min (Fig. 3A). This phenomenon corresponded to the degradation and/or disruption of algal flagella (Movie 3). The flagella no longer functioned correctly, which caused erratic swimming of the algae (Video 3, left cell). This was followed by a complete cessation of swimming. When the flagellum detached from the algae (Video 3, right cell), the attack occurred. With starved *V. atlanticus* LGP32 (60 h of culture in Zobell medium), algae immobilization was fast and significant (91.4% in 15 min, Fig. 3A), and algae were attacked individually being targeted by groups of *V. atlanticus* LGP32 (Movie 4). The percentage of cells attacked and killed peaked at 30% after 15–30 min of contact (Fig. 3B) and then decreased. After 1 h, attacks had stopped with approximately 40% of the algal cells still alive (Fig. 3C). Although it remains unclear whether the attacks occur during a specific phase of growth, it is evident that the cells are already weakened before attack as they have all lost their flagella. An old-starved culture of *V. atlanticus* LGP32 (126 h) significantly immobilized *A. pacificum* ACT03 cells within a few minutes, with lysis occurring immediately (Fig. 3A, C), making it impossible to detect attacks by *V. atlanticus* LGP32 (Fig. 3B). The lysis phase corresponded to initial vesicle formation followed by the bursting of *A. pacificum* ACT03 cells (Movie 5) and was induced by the old-starved culture supernatant of *V. atlanticus* LGP32 (Fig. S1).

We next tested whether this lytic effect was mediated by thermostable molecule (s) secreted by *Vibrio*. The culture supernatant of starved culture of *V. atlanticus* LGP32 (36 h) filtered through a 10 kDa membrane and then incubated at 100°C for 30 min still possessed its lytic properties, indicating that the algicidal compounds produced by *V. atlanticus* LGP32 are small thermostable molecules unlikely to be lytic enzymes, or lysins able to digest the algae cell. However, these experimental observations clearly show the key role of nutrient limitation in triggering the ‘group-attack’ behaviour and the secretion of lytic compounds of *V. atlanticus* LGP32.

Group attack occurs on *A. pacificum* ACT03 in exponential phase of growth.

Here, we wondered whether the live/dead status of algae is important for *V. atlanticus* LGP32-mediated group attacks targeting. To this aim, *A. pacificum* ACT03 in exponential growth phase was first exposed for 30 min to supernatant from 60 hours starved *V. atlanticus* LGP32 Zobell media that induced 25% lysis of *A. pacificum* ACT03 cells and next to the corresponding *V. atlanticus* LGP32 cells. Group attacks were observed on non-degraded *A. pacificum* ACT03 cells, but not on lysed cells. This result is similar to what is observed on the Movie 1 with flash attacks only on immobilized, but not degraded *A. pacificum* ACT03 cells (red), and not on lysed cells (green). In addition, no group attacks occurred on cells from an old *A. pacificum* ACT03 culture (1-month culture). Together, with the very short duration of group attacks (Movie 1), these results indicate that *V. atlanticus* LGP32 group-attacked exponentially growing cells of *A. pacificum* ACT03, but not decomposing algae, suggesting that this behaviour is not just an opportunistic response of heterotrophic bacteria to organic substrates.

Group attack is independent of quorum sensing.

Considering the coordinated action of *V. atlanticus* LGP32 in attacks on *A. pacificum* ACT03, we tested whether the group-attack process depended on the key physiological mechanism that regulates many functions in marine microbial cells, quorum sensing (QS) (Lami, 2019; Papenfort and Bassler, 2016), a type of cell-cell communication. Although QS is a cell-density-dependent mechanism, our results showed no attack from a 12 h culture of *V. atlanticus* LGP32 up to a concentration of 4.10^6 *Vibrio* mL^{-1} (Fig 4A). Attacks were only observed with *V. atlanticus* LGP32 from a 60 h culture at low concentration of 5.10^3 *Vibrio* mL^{-1} to the highest concentration tested of 5.10^5 *Vibrio* mL^{-1} (Fig 4A), consistent with the hypothesis that the attacks were independent of *Vibrio* density.

406 The analysis of the expression of genes involved in the known QS pathways in *Vibrio* cell (Fig. S3A),
407 highlighted that only the AI-2 pathway was induced during nutrient stress of *V. atlanticus* LGP32, because
408 only the expression of the AI synthase (*LuxS*) and its receptor (*LuxP*) increased significantly (Fig. 4B;
409 ANOVA $p < 0.05$). This was confirmed by a QS bioluminescence assay, which showed a AI-2 molecules
410 (unquantified) in the Zobell culture supernatant of *V. atlanticus* LGP32 after 60 h of culture but not after
411 12 h of culture and not in the ENSW supernatant of *V. atlanticus* LGP32 after 12 or 60 h of culture.
412 UHPLC-HRMS/MS provided no evidence of detectable HAI-1) and CAI-1 in any experiments.
413 By targeted mutagenesis of key genes involved in QS pathways Δ*luxM* (HAI-1 production), Δ*luxS* (AI-2
414 production) and Δ*luxR* (high-density QS master regulator) did not lead to any change in the group-attack
415 behaviour of *V. atlanticus* LGP32 (Fig. 4C). Taken together these results showed that group-attack by *V.*
416 *atlanticus* LGP32 is not coordinated by QS.

417 **Group attack related to the availability of iron**.
418 The comparative analysis of the proteome of *V. atlanticus* LGP32 incubated 60 h in artificial seawater
419 (ENSW) versus *V. atlanticus* LGP32 grown 12 h in Zobell nutrient-rich medium revealed 10 proteins
420 modulated by nutrient stress (Fig. S2). The two most down-regulated proteins correspond to be ß-
421 ketoacyl-(acyl-carrier-protein) synthase II (-22-fold in ENSW compared to Zobell), a key regulator of
422 bacterial fatty acid synthesis, and the dihydroorotase (-6.6-fold in ENSW compared to Zobell), an enzyme
423 essential for pyrimidine biosynthesis and thus bacterial proliferation and growth. The low expression of
424 these proteins in ENSW is consistent with *V. atlanticus* LGP32 nutritional starvation. The most up-
425 regulated protein in starved *V. atlanticus* LGP32, with an increase of more than 6-fold, was glucosamine-
426 6-phophate deaminase, an enzyme involved in bacterial energy metabolism probably necessary for its
427 survival. Among the other up -regulated proteins, one was an iron siderophore-binding protein (Spot 4413,
428 Fig. S2A) corresponding to the vibrioferrin outer membrane receptor PvuB, whose gene is part of the *pvu*
429 operons involved in iron transport (Fig. S3B). Interestingly, the corresponding gene *pvuB* as well as the

vibrioferrin membrane receptor gene *pvuA2* (Fig. S3B) were both significantly induced in *Vibrio* under nutrient stress (Fig. 4B; ANOVA $p < 0.01$) but not the one involved in the vibrioferrin biosynthesis, *pvsA* (Fig. 4B). Remarkably, among the 10 proteins identified by proteomic analysis only *V. atlanticus* LGP32 mutant lacking *pvuB* failed to attack *A. pacificum* ACT03 (Fig. 4C; ANOVA $p < 0.001$). In the absence of the *pvuB* gene, *V. atlanticus* LGP32 was unable to attack in group *A. pacificum* ACT03. In addition, *V. atlanticus* LGP32 cells that had been washed with ENSW to remove their culture supernatant metabolites also failed to attack *A. pacificum* ACT03 (Fig. 4C; ANOVA $p < 0.001$), which is congruent with the hypothesis that attacks depend on the *V. atlanticus* LGP32 vibrioferrin transport system. Finally, group-attacks increased significantly, when $FeCl_3$ was added to the *Vibrio* culture medium (Fig. 4D) but not with H_3BO_4 (Fig. 4D). Taken together, those results are consistent with the hypothesis that attacks are regulated by iron.

Group attack is a *Vibrio spp.* behavior specific to *Alexandrium spp.*

To evaluate the dinoflagellates specificity of the group-attack behaviour, a selection of *Vibrio spp.* was co-cultured with a selection of dinoflagellate strains commonly found in the Mediterranean Sea. The results showed that, among the *Vibrio spp.* tested (pathogenic or not) all, under nutrient stress, were able to secrete algicidal compounds, immobilize, 'group-attack' and lyse *A. pacificum* ACT03 cells (Table 1) and no tropism linked to their pathogenesis for fish of invertebrates was observed (Table 1). Among the sixteen dinoflagellates species tested, all eight *Alexandrium spp.* (non-toxic and paralytic shellfish toxin (PST) producers) and *Gymnodinium catenatum* (PST producer) were immobilized, 'group-attacked' and lysed by *V. atlanticus* LGP32 (Table 2), but no tropism linked to PSTs was revealed (Table 2).

DISCUSSION

Predation is a widespread mode of interaction for survival in the natural world (Finke and Denno, 2004; Sinclair et al., 2003). Among predators, predatory bacteria are found in a wide variety of environments,

and like bacteriophages and predatory protists, they have been reported to prey exclusively on other bacteria (Johnke et al., 2014; Perez et al., 2016). Considering predator as a free organism that feeds at the expense of another, this study is the first evidence of the capacity of some *Vibrio* to develop a predatory strategy against an alga. This behaviour differs from parasitism, because the survival of *Vibrio* is not exclusively dependent on the algae.

The strategy developed by *Vibrio* to kill algae may be reminiscent of strategies previously described in the prokaryotes (Johnke et al., 2014). As shown in Movie 1, the interaction between *V. atlanticus* LGP32 and *A. pacificum* ACT03 proceeds in three stages (Fig. 5). The first stage, the '**immobilization stage**', recalls the strategy used by *Streptomyces* to immobilize its prey (Kumbhar et al., 2014) based on the secretion of algicidal metabolites that disrupt the flagella. The second stage, the '**attack stage**', resembles the 'wolf-pack attack' strategy described for *Myxococcus xanthus* and *Lysobacter* (Martin, 2002; Perez et al., 2014). *V. atlanticus* LGP32 also surrounds *A. pacificum* ACT03 cells at high density for a very short time, but does not invade the algal cell. This phenomenon is comparable to that of bacteria clustering around lysed ciliate cells (Blackburn et al., 1998). The third stage, the '**killing stage**', is similar to that of epibiotic bacterial predators, which induces the lysis of bacteria from the outside (Rashidan and Bird, 2001). Overall, these observations show that *V. atlanticus* LGP32 is able of wolf-pack hunting behaviour.

Results showed that quorum sensing does not control algal predation by *Vibrio*, in contrast to iron acquisition systems, which play a major role in regulating this phenotype, as we demonstrated genetically. Indeed, our quorum sensing mutants exhibited the same predatory phenotype as the wild-type *Vibrio atlanticus* LGP32, whereas mutants impaired in iron uptake completely lost this phenotype. However, quorum sensing and iron acquisition are sometimes interconnected in *Vibrio* (McRose et al., 2018). For instance, in *Vibrio vulnificus*, the production of vulnibactin (a siderophore) is controlled by AI-2 (Kim and Shin, 2011). Whether the production of AI-2 by *V. atlanticus* LGP32, induced during group attacks of *A. pacificum* ACT03, promotes the production of vibrioferrin (Lami, 2019) remains to be investigated.

We further show that the group-attack behaviour of *V. atlanticus* LGP32 depends on iron availability. Iron is an essential element for growth in most organisms, including phytoplankton (Martin and Fitzwater, 1988) and bacteria (Neilands, 1981), and its concentration in seawater is known to be very low with measurements in the open ocean surface at 0.2 nM and in deep waters at 0.6 nM (Millero, 1998). Moreover, Its low solubility in seawater limits its availability (Bruland et al., 1994; Wu and Luther, 1994). To acquire iron, bacteria have developed systems based on the secretion (and subsequent uptake) of iron-chelating siderophores to obtain this element from the environment (Amin et al., 2009a). Therefore, many *Vibrio spp*. produce a siderophore known as vibrioferrin, which is synthesized and secreted by proteins encoded by the *pvsABCDE* gene cluster (Fig. S3). Boron being known to be a regulator or capable of being transported by vibrioferrin (Romano et al., 2013; Weerasinghe et al., 2013) we tested its potential involvement in the interaction but no effect was evidenced here. For iron-vibrioferrin uptake, *Vibrio parahaemolyticus* uses a membrane siderophore receptor, called PvuA, which is coupled to an inner membrane ATP-binding cassette (ABC). This ABC transporter system comprised of proteins encoded by the pvuABCDE gene cluster (Fig. S3) is required for transporting the siderophore across the inner membrane (Tanabe et al., 2003). Siderophores are not only iron carriers but also important regulators of virulence (Miethke and Marahiel, 2007) and mediators of bacterial interaction with phytoplankton (Amin et al., 2009b; Kramer et al., 2020). We showed here a pivotal role of iron in the interaction between *V. altlanticus* LGP32 and *A. pacificum* ACT03. This mirrors the mutualistic interaction observed between *Gymnodinium catenatum* and *Marinobacter* (Amin et al., 2009b). In fact, in natural settings, the co-occurence of *Marinobacter* and *G. catenatum* is suggested to depend on a mutually beneficial utilization of iron and carbon resources (Bolch et al., 2011). As in the present study, iron seems to play a key role in the interaction. Indeed, the labile iron released through the photolysis of ferric chelates with vibrioferrin providing a crucial iron source for phytoplankton, which need substantial amounts of iron to support carbon fixation through photosynthesis (Amin et al., 2009a; Yang et al., 2021). This fixed carbon, in turn, sustains the growth of both the phytoplankton and their bacterial counterparts (Amin et al., 2009b; Kramer

et al., 2020). Future study could demonstrate further the role of vibrioferrin in group attack, by adding iron-saturated vibrioferrin to algae-*Vibrio* co-cultures.

In the natural environment, associations between bacteria and algae have already been observed (Lopez-Joven et al., 2018; Miller et al., 2005; Rosales et al., 2022; Xu et al., 2022). Although we do not have definitive proof of a predator/prey interaction *in situ* due to confounding environmental variables, environmental data acquired in the Thau Lagoon showed a correlation between *Alexandrium* and *Vibrio* occurrence, suggesting that such interaction could occur in nature. Evolution of such a predatory behavior would provide an important ecological advantage to *Vibrio* to obtain nutrients in environment, where *Alexandrium spp*. and *Gymnodinium catenatum* form blooms.
With more than 30 species distributed all over the world (Anderson et al., 2012; Hallegraeff et al., 2021), *Alexandrium spp.* and *Gymnodinium spp*. considered as invasive species by the Delivering Alien Invasive Species Inventories for Europe (http://www.europe-aliens.org)), could play an unexpected and important role in maintaining, structuring and regulating *Vibrio* populations in the ecosystem. In turn, *Vibrio* could contribute to the regulation and control of their blooms.

To conclude, this study reveals the capacity of some *Vibrio spp*. to be facultative predators that hunt specific algae. In the current context of climate change favourable to their development monitoring the invasive algae, *Alexandrium spp*. and *Gymnodinium catenatum* should be considered not only for their potent harmful effect on humans and animals, but also as a potential source of nutrients for the expansion of *Vibrio*, particularly pathogenic species (Lemire et al., 2015).

DATA AVAILABILITY

All data on environmental study are included in the article and/or supporting information files. All other study data are available on request from the corresponding author.

REFERENCES

Abadie, E., Amzil, Z., Belin, C., Comps, M.A., Elzière-Papayanni, P., Lassus, P., le Bec, C., Baut, M.L., Nezan, E., Poggi, R., n.d. Contamination de l'étang de Thau par Alexandrium tamarense (No. Rapport 884). Ifremer.

Abadie, E., Kaci, L., Berteaux, T., Hess, P., Sechet, V., Masseret, E., Rolland, J.L., Laabir, M., 2015. Effect of Nitrate, Ammonium and Urea on Growth and Pinnatoxin G Production of Vulcanodinium rugosum. Mar. Drugs 13, 5642–5656. https://doi.org/10.3390/md13095642

Amin, S.A., Green, D.H., Hart, M.C., Kuepper, F.C., Sunda, W.G., Carrano, C.J., 2009a. Photolysis of iron-siderophore chelates promotes bacterial-algal mutualism. Proc. Natl. Acad. Sci. U. S. A. 106, 17071–17076. https://doi.org/10.1073/pnas.0905512106

Amin, S.A., Green, D.H., Kuepper, F.C., Carrano, C.J., 2009b. Vibrioferrin, an Unusual Marine Siderophore: Iron Binding, Photochemistry, and Biological Implications. Inorg. Chem. 48, 11451–11458. https://doi.org/10.1021/ic9016883

Anderson, D.M., Alpermann, T.J., Cembella, A.D., Collos, Y., Masseret, E., Montresor, M., 2012. The globally distributed genus Alexandrium: Multifaceted roles in marine ecosystems and impacts on human health. Harmful Algae 14, 10–35. https://doi.org/10.1016/j.hal.2011.10.012

Baker-Austin, C., Trinanes, J., Gonzalez-Escalona, N., Martinez-Urtaza, J., 2017. Non-Cholera Vibrios: The Microbial Barometer of Climate Change. Trends Microbiol. 25, 76–84. https://doi.org/10.1016/j.tim.2016.09.008

Ben-Gharbia, H., Yahia, O.K.-D., Amzil, Z., Chomerat, N., Abadie, E., Masseret, E., Sibat, M., Triki, H.Z., Nouri, H., Laabir, M., 2016. Toxicity and Growth Assessments of Three Thermophilic Benthic Dinoflagellates (Ostreopsis cf. ovata, Prorocentrum lima and Coolia monotis) Developing in the Southern Mediterranean Basin. Toxins 8, 297. https://doi.org/10.3390/toxins8100297

Blackburn, N., Fenchel, T., Mitchell, J., 1998. Microscale nutrient patches in planktonic habitats shown by chemotactic bacteria. Science 282, 2254–2256. https://doi.org/10.1126/science.282.5397.2254

Bolch, C.J.S., Subramanian, T.A., Green, D.H., 2011. THE TOXIC DINOFLAGELLATE *GYMNODINIUM CATENATUM* (DINOPHYCEAE) REQUIRES MARINE BACTERIA FOR GROWTH[1]. J. Phycol. 47, 1009–1022. https://doi.org/10.1111/j.1529-8817.2011.01043.x

Bruland, K., Orians, K., Cowen, J., 1994. Reactive Trace-Metals in the Stratified Central North Pacific. Geochim. Cosmochim. Acta 58, 3171–3182. https://doi.org/10.1016/0016-7037(94)90044-2

Brumfield, K.D., Usmani, M., Chen, K.M., Gangwar, M., Jutla, A.S., Huq, A., Colwell, R.R., 2021. Environmental parameters associated with incidence and transmission of pathogenic *Vibrio spp* . Environ. Microbiol. 23, 7314–7340. https://doi.org/10.1111/1462-2920.15716

Burkholder, J.M., Shumway, S.E., Glibert, P.M., 2018. Food Web and Ecosystem Impacts of Harmful Algae, in: Harmful Algal Blooms. John Wiley & Sons, Ltd, pp. 243–336. https://doi.org/10.1002/9781118994672.ch7

Burnham, K.P., Anderson, D.R. (Eds.), 2002. Summary, in: Model Selection and Multimodel Inference: A Practical Information-Theoretic Approach. Springer, New York, NY, pp. 437–454. https://doi.org/10.1007/978-0-387-22456-5_8

Chai, Z.Y., Wang, H., Deng, Y., Hu, Z., Tang, Y.Z., 2020. Harmful algal blooms significantly reduce the resource use efficiency in a coastal plankton community. Sci. Total Environ. 704, 135381. https://doi.org/10.1016/j.scitotenv.2019.135381

Coyne, K.J., Wang, Y., Johnson, G., 2022. Algicidal Bacteria: A Review of Current Knowledge and Applications to Control Harmful Algal Blooms. Front. Microbiol. 13, 871177. https://doi.org/10.3389/fmicb.2022.871177

572 Drebes Dörr, N.C., Blokesch, M., 2020. Interbacterial competition and anti-predatory behaviour of
573 environmental *Vibrio cholerae* strains. Environ. Microbiol. 22, 4485–4504.
574 https://doi.org/10.1111/1462-2920.15224
575 Espinoza-Vergara, G., Hoque, M.M., McDougald, D., Noorian, P., 2020. The Impact of Protozoan
576 Predation on the Pathogenicity of Vibrio cholerae. Front. Microbiol. 11, 17.
577 https://doi.org/10.3389/fmicb.2020.00017
578 Fertouna-Bellakhal, M., Dhib, A., Fathalli, A., Bellakhal, M., Chomérat, N., Masseret, E., Laabir, M., Turki,
579 S., Aleya, L., 2015. Alexandrium pacificum Litaker sp. nov (Group IV): Resting cyst distribution and
580 toxin profile of vegetative cells in Bizerte Lagoon (Tunisia, Southern Mediterranean Sea). Harmful
581 Algae 48, 69–82. https://doi.org/10.1016/j.hal.2015.07.007
582 Finke, D.L., Denno, R.F., 2004. Predator diversity dampens trophic cascades. Nature 429, 407–410.
583 https://doi.org/10.1038/nature02554
584 Gay, M., Renault, T., Pons, A.M., Le Roux, F., 2004. Two Vibrio splendidus related strains collaborate to
585 kill Crassostrea gigas: taxonomy and host alterations. Dis. Aquat. Organ. 62, 65–74.
586 https://doi.org/10.3354/dao062065
587 Genovesi, B., Shin-Grzebyk, M.-S., Grzebyk, D., Laabir, M., Gagnaire, P.-A., Vaquer, A., Pastoureaud, A.,
588 Lasserre, B., Collos, Y., Berrebi, P., Masseret, E., 2011. Assessment of cryptic species diversity
589 within blooms and cyst bank of the Alexandrium tamarense complex (Dinophyceae) in a
590 Mediterranean lagoon facilitated by semi-multiplex PCR. J. Plankton Res. 33, 405–414.
591 https://doi.org/10.1093/plankt/fbq127
592 Hadjadji, I., Laabir, M., Frihi, H., Collos, Y., Shao, Z.J., Berrebi, P., Abadie, E., Amzil, Z., Chomérat, N.,
593 Rolland, J.L., Rieuvilleneuve, F., Masseret, E., 2020. Unsuspected intraspecific variability in the
594 toxin production, growth and morphology of the dinoflagellate Alexandrium pacificum R.W.
595 Litaker (Group IV) blooming in a South Western Mediterranean marine ecosystem, Annaba Bay
596 (Algeria). Toxicon 180, 79–88. https://doi.org/10.1016/j.toxicon.2020.04.005
597 Hallegraeff, G.M., Anderson, D.M., Belin, C., Bottein, M.-Y.D., Bresnan, E., Chinain, M., Enevoldsen, H.,
598 Iwataki, M., Karlson, B., McKenzie, C.H., Sunesen, I., Pitcher, G.C., Provoost, P., Richardson, A.,
599 Schweibold, L., Tester, P.A., Trainer, V.L., Yñiguez, A.T., Zingone, A., 2021. Perceived global
600 increase in algal blooms is attributable to intensified monitoring and emerging bloom impacts.
601 Commun. Earth Environ. 2, 117. https://doi.org/10.1038/s43247-021-00178-8
602 Harrison, P., Waters, R., Taylor, F., 1980. A Broad-Spectrum Artificial Seawater Medium for Coastal and
603 Open Ocean Phytoplankton. J. Phycol. 16, 28–35. https://doi.org/10.1111/j.1529-
604 8817.1980.tb00724.x
605 Johnke, J., Cohen, Y., de Leeuw, M., Kushmaro, A., Jurkevitch, E., Chatzinotas, A., 2014. Multiple micro-
606 predators controlling bacterial communities in the environment. Curr. Opin. Biotechnol. 27, 185–
607 190. https://doi.org/10.1016/j.copbio.2014.02.003
608 Johnson, C.N., 2013. Fitness Factors in Vibrios: a Mini-review. Microb. Ecol. 65, 826–851.
609 https://doi.org/10.1007/s00248-012-0168-x
610 Kim, C.M., Shin, S.H., 2011. Modulation of Iron-Uptake Systems by a Mutation of luxS Encoding an
611 Autoinducer-2 Synthase in Vibrio vulnificus. Biol. Pharm. Bull. 34, 632–637.
612 https://doi.org/10.1248/bpb.34.632
613 Kitatsukamoto, K., Oyaizu, H., Nanba, K., Simidu, U., 1993. Phylogenetic-Relationships of Marine-
614 Bacteria, Mainly Members of the Family Vibrionaceae, Determined on the Basis of 16s
615 Ribosomal-Rna Sequences. Int. J. Syst. Bacteriol. 43, 8–19. https://doi.org/10.1099/00207713-
616 43-1-8

617 Kramer, J., Oezkaya, O., Kuemmerli, R., 2020. Bacterial siderophores in community and host interactions.
618 Nat. Rev. Microbiol. 18, 152–163. https://doi.org/10.1038/s41579-019-0284-4
619 Kumbhar, C., Mudliar, P., Bhatia, L., Kshirsagar, A., Watve, M., 2014. Widespread predatory abilities in
620 the genus Streptomyces. Arch. Microbiol. 196, 235–248. https://doi.org/10.1007/s00203-014-
621 0961-7
622 Laabir, M., Jauzein, C., Genovesi, B., Masseret, E., Grzebyk, D., Cecchi, P., Vaquer, A., Perrin, Y., Collos, Y.,
623 2011. Influence of temperature, salinity and irradiance on the growth and cell yield of the
624 harmful red tide dinoflagellate Alexandrium catenella colonizing Mediterranean waters. J.
625 Plankton Res. 33, 1550–1563. https://doi.org/10.1093/plankt/fbr050
626 Laanaia, N., Vaquer, A., Fiandrino, A., Genovesi, B., Pastoureaud, A., Cecchi, P., Collos, Y., 2013. Wind and
627 temperature controls on Alexandrium blooms (2000-2007) in Thau lagoon (Western
628 Mediterranean). Harmful Algae 28, 31–36. https://doi.org/10.1016/j.hal.2013.05.016
629 Labreuche, Y., Le Roux, F., Henry, J., Zatylny, C., Huvet, A., Lambert, C., Soudant, P., Mazel, D., Nicolas, J.-
630 L., 2010. Vibrio aestuarianus zinc metalloprotease causes lethality in the Pacific oyster
631 Crassostrea gigas and impairs the host cellular immune defenses. Fish Shellfish Immunol. 29,
632 753–758. https://doi.org/10.1016/j.fsi.2010.07.007
633 Lami, R., 2019. Quorum Sensing in Marine Biofilms and Environments, in: Quorum Sensing, Academic
634 Press. Elsevier, pp. 55–96. https://doi.org/10.1016/B978-0-12-814905-8.00003-4
635 Le Roux, F., Binesse, J., Saulnier, D., Mazel, D., 2007. Construction of a *Vibrio splendidus* Mutant Lacking
636 the Metalloprotease Gene *vsm* by Use of a Novel Counterselectable Suicide Vector. Appl.
637 Environ. Microbiol. 73, 777–784. https://doi.org/10.1128/AEM.02147-06
638 Leblad, B.R., Amnhir, R., Reqia, S., Sitel, F., Daoudi, M., Marhraoui, M., Abdellah, M.K.O., Veron, B., Er-
639 Raioui, H., Laabir, M., 2020. Seasonal variations of phytoplankton assemblages in relation to
640 environmental factors in Mediterranean coastal waters of Morocco, a focus on HABs species.
641 Harmful Algae 96, 101819. https://doi.org/10.1016/j.hal.2020.101819
642 Lemire, A., Goudenege, D., Versigny, T., Petton, B., Calteau, A., Labreuche, Y., Le Roux, F., 2015.
643 Populations, not clones, are the unit of vibrio pathogenesis in naturally infected oysters. Isme J.
644 9, 1523–1531. https://doi.org/10.1038/ismej.2014.233
645 LeRoux, F., Wegner, K.M., Baker-Austin, C., Vezzulli, L., Osorio, C.R., Amaro, C., Ritchie, J.M., Defoirdt, T.,
646 Destoumieux-Garzon, D., Blokesch, M., Mazel, D., Jacq, A., Cava, F., Gram, L., Wendling, C.C.,
647 Strauch, E., Kirschner, A., Huehn, S., 2015. The emergence of Vibrio pathogens in Europe:
648 ecology, evolution, and pathogenesis (Paris, 11-12th March 2015). Front. Microbiol. 6, 830.
649 https://doi.org/10.3389/fmicb.2015.00830
650 Li, D., Zhang, H., Fu, L., An, X., Zhang, B., Li, Y., Chen, Z., Zheng, W., Yi, L., Zheng, T., 2014. A Novel
651 Algicide: Evidence of the Effect of a Fatty Acid Compound from the Marine Bacterium, Vibrio sp
652 BS02 on the Harmful Dinoflagellate, Alexandrium tamarense. Plos One 9, e91201.
653 https://doi.org/10.1371/journal.pone.0091201
654 Liu, P.-C., Lee, K.-K., Yii, K.-C., Kou, G.-H., Chen, S.-N., 1996. News & Notes: Isolation of Vibrio harveyi
655 from Diseased Kuruma Prawns Penaeus japonicus. Curr. Microbiol. 33, 129–132.
656 https://doi.org/10.1007/s002849900087
657 Lopez-Joven, C., Rolland, J.-L., Haffner, P., Caro, A., Roques, C., Carre, C., Travers, M.-A., Abadie, E.,
658 Laabir, M., Bonnet, D., Destoumieux-Garzon, D., 2018. Oyster Farming, Temperature, and
659 Plankton Influence the Dynamics of Pathogenic Vibrios in the Thau Lagoon. Front. Microbiol. 9,
660 2530. https://doi.org/10.3389/fmicb.2018.02530

661 Mandel, M.J., Stabb, E.V., Ruby, E.G., 2008. Comparative genomics-based investigation of resequencing
662 targets in Vibrio fischeri: Focus on point miscalls and artefactual expansions. Bmc Genomics 9,
663 138. https://doi.org/10.1186/1471-2164-9-138
664 Marampouti, C., Buma, A.G.J., De Boer, M.K., 2021. Mediterranean alien harmful algal blooms: origins
665 and impacts. Environ. Sci. Pollut. Res. 28, 3837–3851. https://doi.org/10.1007/s11356-020-
666 10383-1
667 Martin, J., Fitzwater, S., 1988. Iron-Deficiency Limits Phytoplankton Growth in the Northeast Pacific
668 Subarctic. Nature 331, 341–343. https://doi.org/10.1038/331341a0
669 Martin, M.O., 2002. Predatory prokaryotes: An emerging research opportunity. J. Mol. Microbiol.
670 Biotechnol. 4, 467–477.
671 Mavian, C., Paisie, T.K., Alam, M.T., Browne, C., Beau De Rochars, V.M., Nembrini, S., Cash, M.N., Nelson,
672 E.J., Azarian, T., Ali, A., Morris, J.G., Salemi, M., 2020. Toxigenic Vibrio cholerae evolution and
673 establishment of reservoirs in aquatic ecosystems. Proc. Natl. Acad. Sci. 117, 7897–7904.
674 https://doi.org/10.1073/pnas.1918763117
675 McRose, D.L., Baars, O., Seyedsayamdost, M.R., Morel, F.M.M., 2018. Quorum sensing and iron regulate
676 a two-for-one siderophore gene cluster in *Vibrio harveyi*. Proc. Natl. Acad. Sci. 115, 7581–7586.
677 https://doi.org/10.1073/pnas.1805791115
678 Miethke, M., Marahiel, M.A., 2007. Siderophore-Based Iron Acquisition and Pathogen Control. Microbiol.
679 Mol. Biol. Rev. 71, 413–451. https://doi.org/10.1128/MMBR.00012-07
680 Miller, S.D., Haddock, S.H.D., Elvidge, C.D., Lee, T.F., 2005. Detection of a bioluminescent milky sea from
681 space. Proc. Natl. Acad. Sci. U. S. A. 102, 14181–14184.
682 https://doi.org/10.1073/pnas.0507253102
683 Millero, F.J., 1998. Solubility of Fe(III) in seawater. Earth Planet. Sci. Lett. 154, 323–329.
684 https://doi.org/10.1016/S0012-821X(97)00179-9
685 Muhling, B.A., Jacobs, J., Stock, C.A., Gaitan, C.F., Saba, V.S., 2017. Projections of the future occurrence,
686 distribution, and seasonality of three Vibrio species in the Chesapeake Bay under a high-emission
687 climate change scenario. Geohealth 1, 278–296. https://doi.org/10.1002/2017GH000089
688 Neilands, J., 1981. Iron-Absorption and Transport in Microorganisms. Annu. Rev. Nutr. 1, 27–46.
689 https://doi.org/10.1146/annurev.nu.01.070181.000331
690 Oberbeckmann, S., Fuchs, B.M., Meiners, M., Wichels, A., Wiltshire, K.H., Gerdts, G., 2012. Seasonal
691 Dynamics and Modeling of a Vibrio Community in Coastal Waters of the North Sea. Microb. Ecol.
692 63, 543–551. https://doi.org/10.1007/s00248-011-9990-9
693 Pal, M., Yesankar, P.J., Dwivedi, A., Qureshi, A., 2020. Biotic control of harmful algal blooms (HABs): A
694 brief review. J. Environ. Manage. 268, 110687. https://doi.org/10.1016/j.jenvman.2020.110687
695 Papenfort, K., Bassler, B.L., 2016. Quorum sensing signal-response systems in Gram-negative bacteria.
696 Nat. Rev. Microbiol. 14, 576–588. https://doi.org/10.1038/nrmicro.2016.89
697 Perez, J., Jimenez-Zurdo, J.I., Martinez-Abarca, F., Millan, V., Shimkets, L.J., Munoz-Dorado, J., 2014.
698 Rhizobial galactoglucan determines the predatory pattern of Myxococcus xanthus and protects
699 Sinorhizobium meliloti from predation. Environ. Microbiol. 16, 2341–2350.
700 https://doi.org/10.1111/1462-2920.12477
701 Perez, J., Moraleda-Munoz, A., Javier Marcos-Torres, F., Munoz-Dorado, J., 2016. Bacterial predation: 75
702 years and counting! Environ. Microbiol. 18, 766–779. https://doi.org/10.1111/1462-2920.13171
703 Pfaffl, M.W., 2001. A new mathematical model for relative quantification in real-time RT-PCR. Nucleic
704 Acids Res. 29, e45. https://doi.org/10.1093/nar/29.9.e45
705 Rashidan, K.K., Bird, D.F., 2001. Role of predatory bacteria in the termination of a cyanobacterial bloom.
706 Microb. Ecol. 41, 97–105.

Rodrigues, A.M.S., Lami, R., Escoubeyrou, K., Intertaglia, L., Mazurek, C., Doberva, M., Pérez-Ferrer, P., Stien, D., 2022. Straightforward *N* -Acyl Homoserine Lactone Discovery and Annotation by LC–MS/MS-based Molecular Networking. J. Proteome Res. 21, 635–642. https://doi.org/10.1021/acs.jproteome.1c00849

Rolland, J.-L., Pelletier, K., Masseret, E., Rieuvilleneuve, F., Savar, V., Santini, A., Amzil, Z., Laabir, M., 2012. Paralytic Toxins Accumulation and Tissue Expression of alpha-Amylase and Lipase Genes in the Pacific Oyster Crassostrea gigas Fed with the Neurotoxic Dinoflagellate Alexandrium catenella. Mar. Drugs 10, 2519–2534. https://doi.org/10.3390/md10112519

Romano, A., Trimble, L., Hobusch, A.R., Schroeder, K.J., Amin, S.A., Hartnett, A.D., Barker, R.A., Crumbliss, A.L., Carrano, C.J., 2013. Regulation of iron transport related genes by boron in the marine bacterium Marinobacter algicola DG893. Metallomics 5, 1025. https://doi.org/10.1039/c3mt00068k

Rosales, D., Ellett, A., Jacobs, J., Ozbay, G., Parveen, S., Pitula, J., 2022. Investigating the Relationship between Nitrate, Total Dissolved Nitrogen, and Phosphate with Abundance of Pathogenic Vibrios and Harmful Algal Blooms in Rehoboth Bay, Delaware. Appl. Environ. Microbiol. 88, e00356-22. https://doi.org/10.1128/aem.00356-22

Sinclair, A.R.E., Mduma, S., Brashares, J.S., 2003. Patterns of predation in a diverse predator-prey system. Nature 425, 288–290. https://doi.org/10.1038/nature01934

Su, R.Q., Yang, X.R., Zheng, T.L., Tian, Y., Jiao, N.Z., Cai, L.Z., Hong, H.S., 2007. Isolation and characterization of a marine algicidal bacterium against the toxic dinoflagellate Alexandrium tamarense. Harmful Algae 6, 799–810. https://doi.org/10.1016/j.hal.2007.04.004

Tanabe, T., Funahashi, T., Nakao, H., Miyoshi, S.-I., Shinoda, S., Yamamoto, S., 2003. Identification and Characterization of Genes Required for Biosynthesis and Transport of the Siderophore Vibrioferrin in *Vibrio parahaemolyticus*. J. Bacteriol. 185, 6938–6949. https://doi.org/10.1128/JB.185.23.6938-6949.2003

Thompson, F.L., Thompson, C.C., Swings, J., 2003. Vibrio tasmaniensis sp. nov., isolated from Atlantic Salmon (Salmo salar L.). Syst. Appl. Microbiol. 26, 65–69. https://doi.org/10.1078/072320203322337326

Tourneroche, A., Lami, R., Hubas, C., Blanchet, E., Vallet, M., Escoubeyrou, K., Paris, A., Prado, S., 2019. Bacterial–Fungal Interactions in the Kelp Endomicrobiota Drive Autoinducer-2 Quorum Sensing. Front. Microbiol. 10, 1693. https://doi.org/10.3389/fmicb.2019.01693

Vanhove, A.S., Rubio, T.P., Nguyen, A.N., Lemire, A., Roche, D., Nicod, J., Vergnes, A., Poirier, A.C., Disconzi, E., Bachere, E., Le Roux, F., Jacq, A., Charriere, G.M., Destoumieux-Garzon, D., 2016. Copper homeostasis at the host vibrio interface: lessons from intracellular vibrio transcriptomics. Environ. Microbiol. 18, 875–888. https://doi.org/10.1111/1462-2920.13083

Wang, X., Li, Z., Su, J., Tian, Y., Ning, X., Hong, H., Zheng, T., 2010. Lysis of a red-tide causing alga, Alexandrium tamarense, caused by bacteria from its phycosphere. Biol. Control 52, 123–130. https://doi.org/10.1016/j.biocontrol.2009.10.004

Wang, Y., Li, S., Liu, G., Li, X., Yang, Q., Xu, Y., Hu, Z., Chen, C.-Y., Chang, J.-S., 2020. Continuous production of algicidal compounds against Akashiwo sanguinea via a Vibrio sp. co-culture. Bioresour. Technol. 295, 122246. https://doi.org/10.1016/j.biortech.2019.122246

Weerasinghe, A.J., Amin, S.A., Barker, R.A., Othman, T., Romano, A.N., Parker Siburt, C.J., Tisnado, J., Lambert, L.A., Huxford, T., Carrano, C.J., Crumbliss, A.L., 2013. Borate as a Synergistic Anion for *Marinobacter algicola* Ferric Binding Protein, FbpA: A Role for Boron in Iron Transport in Marine Life. J. Am. Chem. Soc. 135, 14504–14507. https://doi.org/10.1021/ja406609s

752 Wu, J., Luther, G., 1994. Size-Fractionated Iron Concentrations in the Water Column of the Western
753 North-Atlantic Ocean. Limnol. Oceanogr. 39, 1119–1129.
754 https://doi.org/10.4319/lo.1994.39.5.1119
755 Xu, Q., Wang, P., Huangleng, J., Su, H., Chen, P., Chen, X., Zhao, H., Kang, Z., Tang, J., Jiang, G., Li, Z., Zou,
756 S., Dong, K., Huang, Y., Li, N., 2022. Co-occurrence of chromophytic phytoplankton and the Vibrio
757 community during Phaeocystis globosa blooms in the Beibu Gulf. Sci. Total Environ. 805, 150303.
758 https://doi.org/10.1016/j.scitotenv.2021.150303
759 Yang, Q., Feng, Q., Zhang, B., Gao, J., Sheng, Z., Xue, Q., Zhang, X., 2021. Marinobacter alexandrii sp. nov.,
760 a novel yellow-pigmented and algae growth-promoting bacterium isolated from marine
761 phycosphere microbiota. Antonie Van Leeuwenhoek Int. J. Gen. Mol. Microbiol. 114, 709–718.
762 https://doi.org/10.1007/s10482-021-01551-5
763

ACKNOWLEDGMENT

The authors thank F. Le Roux and Y. Labruche for their gift of *Vibrio* mutants; E. Garcés, S. Turki, H. Frehi, A. Bouquet and W. Medhioub for their contribution in obtaining Mediterranean phytoplankton strains; K. Escoubeyrou and D. Stien for advice on HRMS/MS data; V. Diakou-Verdin and E. Jublanc from the Montpellier RIO Imaging Platform for access to microscope facilities (www.mri.cnrs.fr); P. Clair from the Montpellier qPHD platform and the Technoviv platform of the UPVD for access to PCR facilities; N. Brunet, A. Lang, A. Payelleville, T. Milhau and M. Leroy for their technical assistance; The IFREMER LER-LR laboratory for access to the Thau Lagoon; the BIO2MAR platform at the Observatoire Océanologique de Banyuls for providing access to UHPLC-HRMS/MS facilities.

FUNDING

European VIVALDI grant 678589, French EC2CO ROSEOCOM grant and IFREMER ALGOVIR grant.

FIGURES, TABLES and VIDEOS

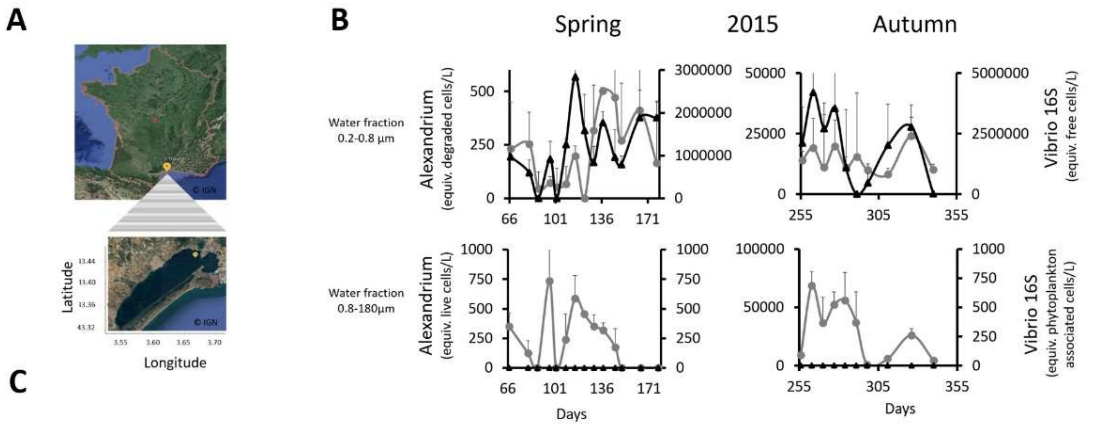

C

Model degraded Alexandrium cells	AICc
Intercept+ free Vibrio	171.77
intercept	172.57
Intercept + salinity	173.41
Intercept + temperature	173.94
Intercept+ free Vibrio + salinity	174.99
Intercept+ free Vibrio + temperature	175.37
Intercept + temperature + salinity	177.72
Intercept+ free Vibrio + temperature + salinity	180.56

D

	Estimate	Std error	T value	Pr(>|t|)
Intercept	235.41	38.69	6.08	7.91×10^{-05}
Vibrio	83.19	40.27	2.07	0.06

Figure 1. Dynamics of *Alexandrium* and *Vibrio* in the environment. (A) Location of the monitoring station in the Thau Lagoon (southern France). **(B)** Mean abundance (DNA equiv.) of *Vibrio spp*. (16S) and Alexandrium *spp*. *(A. pacificum* ACT03 + *A. tamarense* ATT07). *Vibrio* cells (black line with diamond dot) and degraded *Alexandrium* cells (grey line with round dot) were evidence in the 0.2–0.8 µm fraction (free *Vibrio* fraction) in spring and autumn 2015. Living *Alexandrium* cells (grey line with roundot) but no plankton-associated *Vibrio spp*. (black line with diamond dot) were evidence in the 0.8–180 µm in spring and autumn. **(C)** Result of Akaike information criterion (AICc) models tested to explain the mean value of degraded Alexandrium cells (dead cells) in spring. **(D)** Wald test of the AICc model attributing the mean value of degraded cells of Alexandrium in spring to free *Vibrio*.

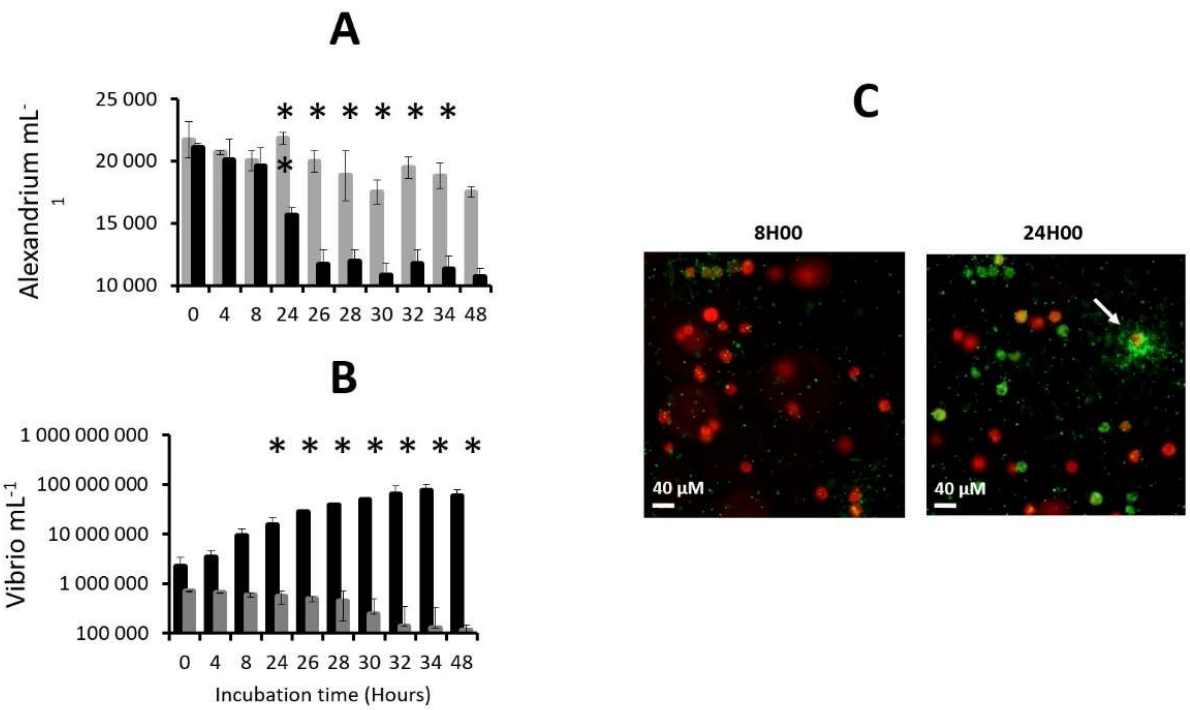

Figure 2. Incubation of *Vibrio atlanticus* LGP32 and *Alexandrium pacificum* ACT03 in enriched natural seawater (ENSW). **(A)** *A. pacificum* ACT03 cultured alone (grey bar) and incubated with *V. atlanticus* LGP32 (black bar) in ENSW. **(B)** *V. atlanticus* LGP32 cultured alone (grey bar) and incubated with *A. pacificum* ACT03 (black bar) in ENSW. **(C)** Images of the interaction of *V. atlanticus* LGP32-GFP with *A. pacificum* ACT03 taken at 8h00 and 28h00 of co-culture. *V. atlanticus* LGP32 (small green cells), living *A. pacificum* ACT03 cells (large red cells) and degraded *A. pacificum* ACT03 cells (large green cells). *P < 0.01 (analysis by pairs).

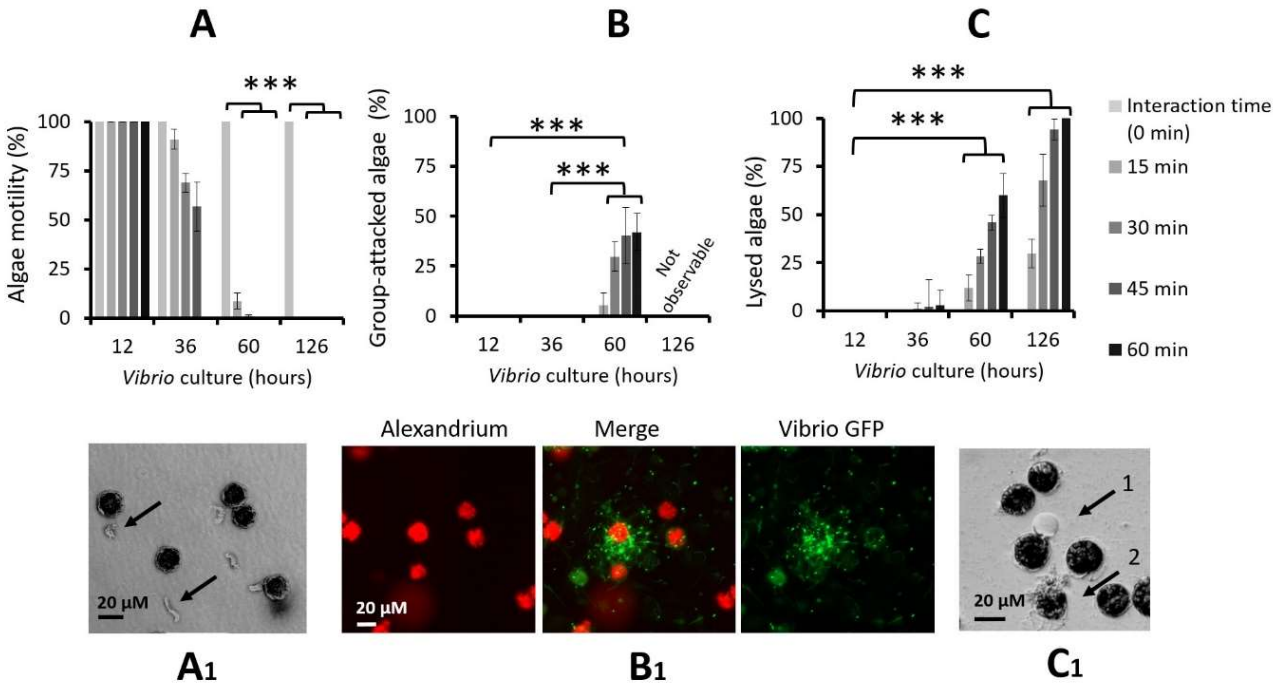

Figure 3. Role of *Vibrio atlanticus* LGP32 starvation in the interspecific interaction process. Experiments were conducted by incubating *A. pacificum* ACT03 with *V. atlanticus* LGP32 previously grown for 12, 36, 60 and 126 h in Zobell medium. **(A)** Percentage of motile *A. pacificum* ACT03. **(B)** *A. pacificum* ACT03 group-attacked by *V. atlanticus* LGP32 and **(C)** *A. pacificum* ACT03 lysis after 0, 15, 30, 45 and 60 min of interaction. Corresponding pictures showing **(A1)** Black arrows indicate unhooked and degrade flagellum from *A. pacificum* ACT03 flagellum, **(B1)** Image of the interaction of *V. atlanticus* LGP32-GFP with *A. pacificum* ACT03 taken at 8h00 of co-culture. *V. atlanticus* LGP32 (small green cells), living *A. pacificum* ACT03 (large red cells) and dead *A. pacificum* ACT03 (large green cell). **(C1)** Black arrow 1 indicate vesicle formation on *A. pacificum* ACT03 cell and black arrow 2 indicate exploded *A. pacificum* ACT03 cell. ***P <0.001.

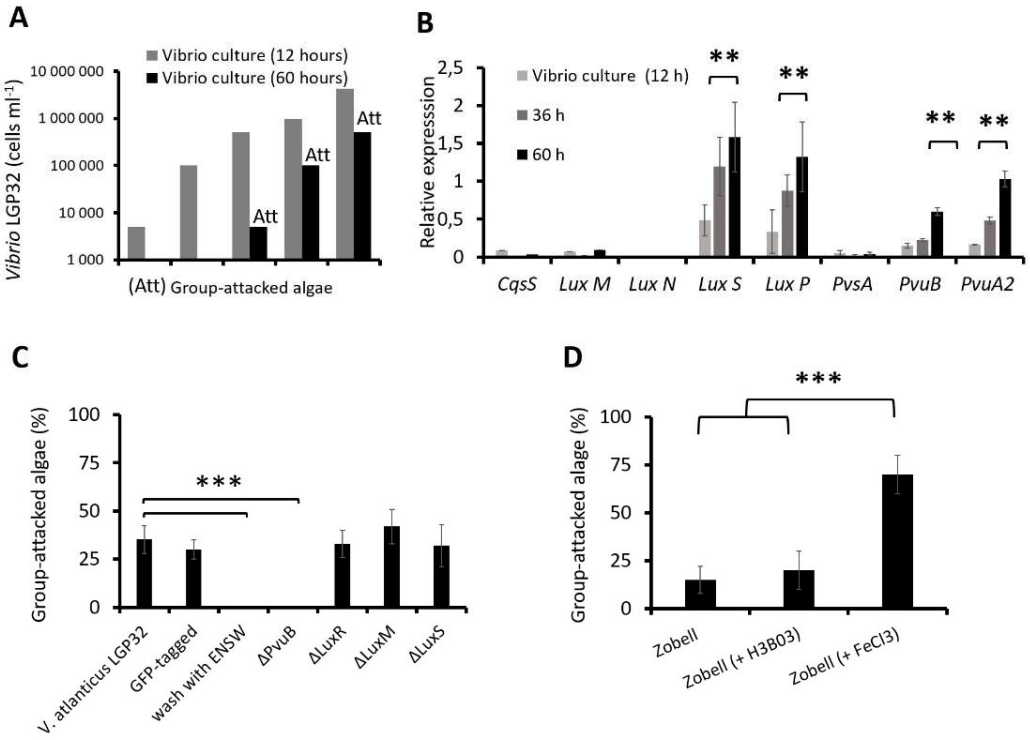

Figure 4. Role of quorum sensing and the vibrioferrin iron uptake pathway in the interaction process. **(A)** Effect of *V. atlanticus* LGP32 cell density on the predation process. Experiments examined the impact of *V. atlanticus* LGP32 cell density on its ability to attack *A. pacificum* ACT03. *A. pacificum* ACT03 cells (2.10^4 cells) were incubated with *V. atlanticus* LGP32 grown for 60 hours in Zobell medium at concentrations ranging from 5×10^3 to 5×10^5 cells mL^{-1} (represented by black bars). For comparison, *A. pacificum* ACT03 was also incubated with *V. atlanticus* LGP32 grown for only 12 hours in Zobell medium at concentrations ranging from 5×10^3 to 4×10^6 cells mL−1 (represented by grey bars). The term "Att" indicates cells of *A. pacificum* ACT03 that were subjected to group attacks by *V. atlanticus* LGP32. **(B)** CqsS, luxM, luxN, luxS, and luxP quorum sensing and PvsA, PvuB and PvuA2 vibrioferrin pathway genes expression in *V. atlanticus* LGP32 grown for 12, 36 and 60 h in Zobell medium. **(C)** Effect of *V. atlanticus* LGP32 mutants on the group-attacked process. Experiments were conducted by incubating *A. pacificum* ACT03 with *V. atlanticus* LGP32, *V. atlanticus* LGP32 tagged with GFP, *V. atlanticus* LGP32 washed with ENSW or *V. atlanticus* LGP32 mutant ΔPvuB, ΔluxM, ΔluxR and ΔluxS previously grown 60 h in Zobell media (control), The percentage of *A. pacificum* ACT03 group-attacked was determined during the first 30 min of exposure. **(D)** Effect of *V. atlanticus* LGP32 cultures media composition on the group-attacked process. Experiments were conducted by incubating *A. pacificum* ACT03 with *V. atlanticus* LGP32 grown 60 h in Zobell media supplemented with H_3BO_4 or $FeCl_3$. The results were compared with an exposure to *V. atlanticus* LGP32 grown 60 h in Zobell media. **P <0.01, ***P <0.001

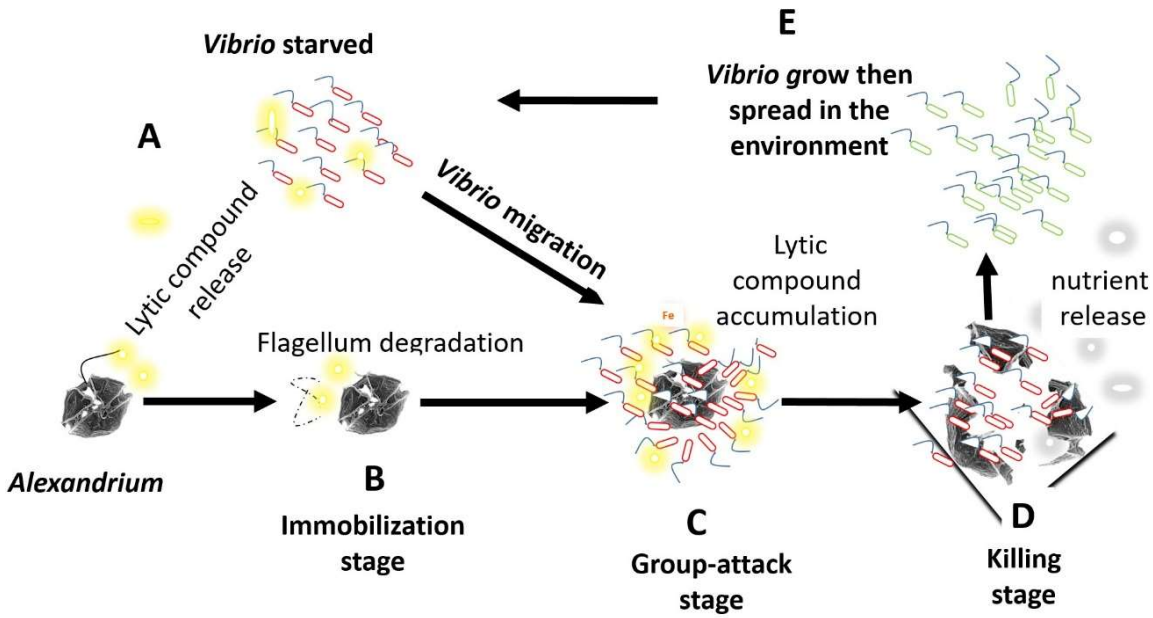

Figure 5. Schematic representation of a putative strategy developed by *Vibrio spp*. to feed on Alexandrium *spp*. and *G. catenatum* in the environment. (A) *Vibrio* in the environment when subjected to starvation secrete non-protein lytic compounds. **(B)** Some of these lytic compounds degrade the flagella, immobilizing the alga (immobilization stage). **(C)** Then *Vibrio* swims and clusters around its prey coordinating group attacks (group-attack stage). **(D)** Lytic compounds released by *Vibrio* where able to concentrate around the algae cells, thereby lysing the algae (killing stage). **(E)** Feeding on the released nutrients, *Vibrio* multiply and then spread in the environment. Yellow clouds: Lytic compound release by *Vibrio,* Grey clouds: Algal nutrients released upon lysis.

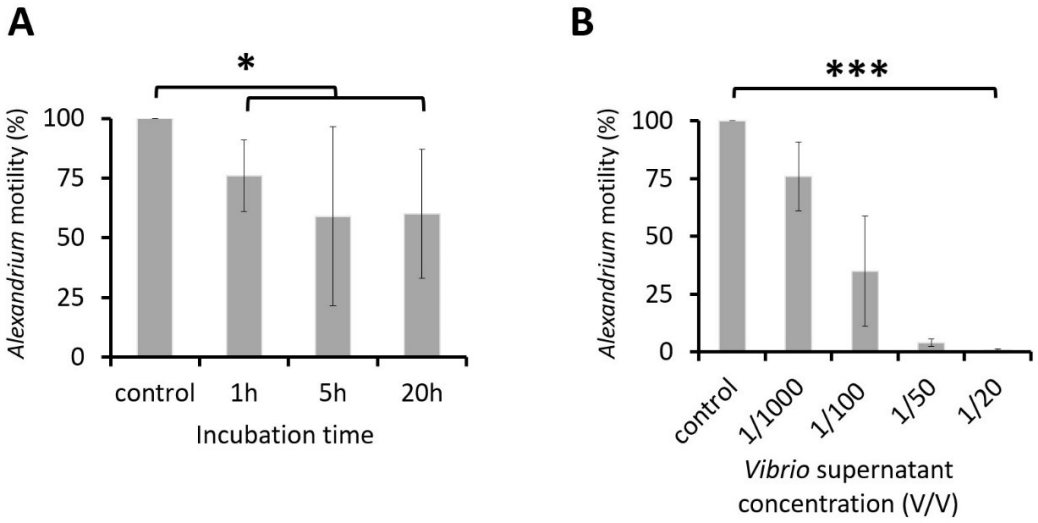

Figure S1.Time and dose-dependent effects of the *V. atlanticus* LGP32 culture supernatant on *A. pacificum* ACT03 motility. (A) A time dependence experiment was conducted by incubating *A. pacificum* ACT03 for 1, 5 or 20 h with 1/1000 v/v (1 µL/mL) of culture supernatant from *V. atlanticus* LGP32 previously grown for 60 h in Zobell culture media. **(B)** A dose dependence experiment was conducted by incubating *A. pacificum* ACT03 for 1 h with 1/1000 to 1/20 v/v (1-50 µL/mL) of culture supernatant from *V. atlanticus* previously grown for 60 h in Zobell media. The percentage of motile *A. pacificum* ACT03 was determined after 1 hours of exposure.*P < 0.05, ***P < 0.001

848

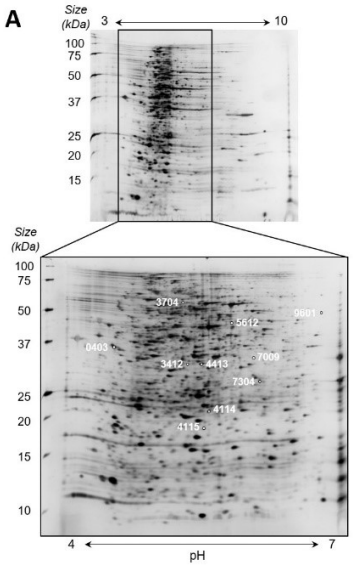

B

Spot #	Value ENSW	Value Zobell	Ratio (ENSW/Zobell)	Best ID Accession	#Peptides	-10logP Prot	-10logP Pept. Min	-10logP Pept. Max	Seq coverage	CDD accession	Best ID Description	Expected mass	Expected pI
7304	3620,4	570,7	6,34	WP_012601215.1	3	172,83	67,81	92,01	14%	PRK00443	glucosamine-6-phosphate deaminase	29610	5,53
4115	1203,8	191,9	6,27	ND									
0403	3697,4	750,2	4,93	WP_004733797.1	16	253,95	23,25	124,97	33%	cd13641	ABC transporter substrate-binding protein	36195	4,52
4413	**640,2**	**267,4**	**2,39**	**WP_012600975.1**	**21**	**241,28**	**25,81**	**101,45**	**51%**	**PRK11411**	**iron siderophore-binding protein, PvuB**	**36111**	**5,73**
7009	616,6	316,3	1,95	ND									
3704	683,2	1303	-1,91	WP_009848030.1	30	360,8	29,21	121,35	54%	PRK09344	phosphoenolpyruvate carboxykinase (ATP)	59755	4,85
4114	315,2	812,6	-2,58	WP_009847387.1	2	58,71	58,71	58,71	8%	PRK00129	uracil phosphoribosyltransferase	22658	5,21
3412	57,7	238,2	-4,13	WP_012604509.1	10	244,21	29,11	105,11	38%	cd13674	C4-dicarboxylate ABC transporter	36946	5,26
5612	211,4	1395,9	-6,60	WP_012600249.1	2	79,11	40,49	40,83	6%	PRK05451	dihydroorotase	37599	5,36
9601	76,9	1717,1	-22,33	WP_004736554.1	12	208,83	33,74	100,38	29%	PRK08722	beta-ketoacyl-(acyl-carrier-protein)synthase II	43007	5,95

849

850 **Figure S2. *Vibrio atlanticus* LGP32 proteome analysis following nutrient stress. (A)** Example of 2D
851 gel, the numbers in white on the gel 4-7 correspond to the number and position of the protein spots
852 analyzed. **(B)** Proteins identified by LC-MS/MS as differentially represented in the 2D gel comparative
853 approach following nutrient stress. ND: Not determined; ENSW (artificial seawater)**.**
854

855

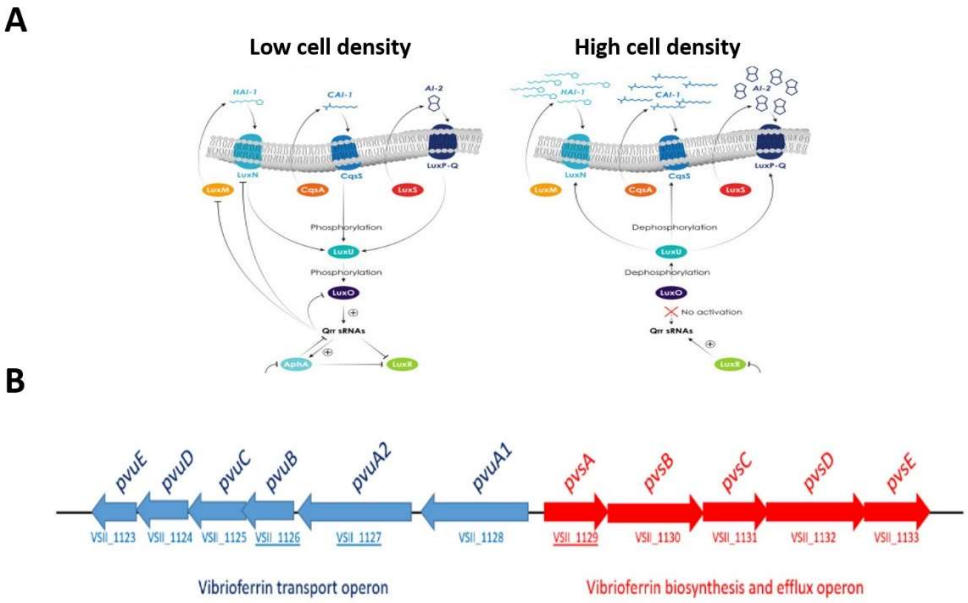

856

857 **Figure S3. Quorum sensing and the vibrioferrin iron uptake pathway in *Vibrio*. (A)** Putative
858 quorum sensing (QS) pathways at low and high cell density in *Vibrio* according to Lami et
859 al.(Lami, 2019). **(B)** Genetic organization of the vibrioferrin utilization gene cluster on *V.*
860 *atlanticus* LGP32 chromosome 2. The Pvu and Pvs operons are involved in the secretion and the
861 transport of ferric vibrioferrin and biosynthesis of vibrioferrin, respectively. Arrows indicate the
862 transcriptional directions of the genes. VSII1126, VSII1137 and VSII1129 corresponding to
863 PvuB, PvuA2 and PvsA genes respectively.
864
865

866 **Table 1.** Ability of Vibrio *spp*. and strains to secrete algicidal compounds and attack *Alexandrium*
867 *pacificum* LGP32 in groups. NT: not determined.

Vibrio species	Strains	Virulence for fish or invertebrates	References	Secretion of algicidal compounds (This study)	Group attack (This study)
Vibrio atlanticus LGP32	WT	+	(Gay et al., 2004)	+	+
//	WT + pSW3654T-GFP	+	(Le Roux et al., 2007)	+	+
//	ΔLuxM	ND	Ifremer Institute, France	+	+
//	ΔLuxS	ND	//	+	+
//	ΔLuxR	ND	//	+	+
//	ΔPvuB	ND	This work	+	-
Vibrio tasmaniensis	J5-9	+	(Lemire et al., 2015)	+	+
//	LMG20012^T	-	(Thompson et al., 2003)	+	+
Vibrio crassostreae	J2.9	+	(Lemire et al., 2015)	+	+
//	J2-8	-	//	+	+
Vibrio fischeri	ES114	ND	(Mandel et al., 2008)	+	+
Vibrio harveyi	ATCC14126	+	(Liu et al., 1996)	+	+
Vibrio aestuarianus	janv-32	+	(Labreuche et al., 2010)	+	+

868

869 **Table 2.** Ability of *Vibrio Atlanticus* LGP32 to degrade flagella, attack in group and lysed the targeted
870 dinoflagellates *spp*. commonly found in the Mediterranean Sea. ND not determined.

Dinoflagellates species	Strains	Toxicity for human	References	Degraded flagella (This study)	Attacked in groups (This study)	Lysed cells (This study)
Alexandrium pacificum	ACT03, Thau, France	+	(Laabir et al., 2011)	+	+	+
Alexandrium catenella	Bizerte, Tunisia	+	(Fertouna-Bellakhal et al., 2015)	+	+	+
//	F3-9F, Tarragona, Spain	ND	//	+	+	+
//	C10-5, Annaba, Algeria	+	(Hadjadji et al., 2020)	+	+	+
Alexandrium tamarense	ATT07, Thau, France	-	(Rolland et al., 2012)	+	+	+
Alexandrium spp.	Golf of Tunis, Tunisia	ND	Algal collection university of Montpellier, France	+	+	+
//	Bizerte, Tunisia	ND	//	+	+	+
//	Mediterranean coast, Morocco	ND	//	+	+	+
Prorocentrum lima	PLBZT14, Bizerte, Tunisia	+	(Ben-Gharbia et al., 2016)	-	-	-
Coolia monotis	CMBZT14, Bizerte, Tunisia	ND	//	-	-	-
Vulcanodinium rugosum	IFR-VRU-01, Ingril, France	+	(Abadie et al., 2015)	-	-	-
Karenia selliformis	Golf of Gabes, Tunisia	NT	Algal collection university of Montpellier, France	-	-	-
Scripsiella trochoidae	Mellah Lagoon, Algeria	-	//	-	-	-
Gyrodinium impudicum	Golf of Tunis, Tunisia	-	//	-	-	-
Amphidium carterae	SAMS, Scotland	NT	SAMS laboratory, Scotland	-	-	-
Gymnodinium catenatum	M'diq Bay, Morocco	+	(Leblad et al., 2020)	+	+	+

871

872 **Table 3.** Oligonucleotide sequences of primers used for RNA expression analysis.

Species	genes	Primers Sequences	Tm (°C)	Efficiency	References
Alexandrium pacificum (ACT03)	18S – 28S rRNA ITS region	TGATATTGTGGGCAACTGTAA AACATCTGTTAGCTCACGGAA	54		(Genovesi et al., 2011)
Alexandrium tamarense (ATT07)	18S – 28S rRNA ITS region	TGGTAATTCTTCATTGATTACAATG AACATCTGTTAGCTCACGGAA	54		//
Vibrios spp.	16S	CGGTGAAATGCGTAGAGAT TTACTAGCGATTCCGAGTTC	62		(Kitatsukamoto et al., 1993)
Vibrio atlanticus LGP32	LuxN (VS_II0260)	CACTTGCTAGTATCATCGC ATCGAGTTAGCAAGAGCAC	60	1,92	This work
//	LuxM (VS_II0261)	TCCACTTATCACAAACAGG ACTGTACTTCCATTTGTCG	60	1,91	//
//	LuxP (VS_II0355)	AAGTTCAGGATGAACCTATC CAAAGAGATACTTTGCTGAG	60	1,89	//
//	LuxS (VS_2562)	ACTCTCGAGCACCTATACG GAAGGCGTACCAATCAAGC	60	1,85	//
//	CqsS (VS_1725)	GACATCTATTGATGTTATGC TCACCCACTTCACGTAACTG	60	1,91	//
//	PvsA (VS_II0355),Vibrioferrin biosynthesis protein	CAGAGCAAGAGCTAGAACC TCGTTGAGAACCTGACGAG	59	1,91	//
//	PvuB (VS_II1126), ABC transporter vibrioferrin uptake FecB	TAGTGCAACCATGGGAATCG TAAACCGTACGTAGACGCTC	57	2,01	//
//	PvuA2 (VS_II1127), Vibrioferrin receptor FecA	GGAGCTACAAGCATTCGTTC TTCGTCATATGGTCGCTTCG	57	2,08	//
//	Housekiping gene 1, CcmC (VS_0852)	ATTGCCGCCTTTATCGGTTT CAAGCACCCCACATTGGTTT	60		(Vanhove et al., 2016)
//	Housekiping gene 2, 6-phosphofructokinase (VS_2913)	GCCGTCACTGTGGTGACCTT TGCTTCTTGCCTTTCGCAAT	60		//

873

VIDEOS

Video 1. Dynamics of *Vibrio atlanticus* LGP32-*Alexandrium pacificum* ACT03 interaction. GFP-tagged *V. atlanticus* (small green cells); living *A. pacificum* (large red cells); degraded *A. pacificum* (large green cells) filmed under an epifluorescence microscope.

Video 2. Second-by-second timing of *Vibrio Atlanticus* LGP32 attacking *Alexandrium pacificum* ACT03. GFP-tagged *V. atlanticus* (small green cells); *A. pacificum* living cell (large red cells) filmed under an epifluorescence microscope**.**

Video 3. Degradation and disruption of *Alexandrium pacificum* ACT03 flagella. Effect of *Vibrio* supernatant on the first stage of the interaction filmed under a confocal microscope.

Video 4. Group attacks of *Vibrio atlanticus* LGP32 on target *Alexandrium pacificum* ACT03. *Vibrio*, filmed under a confocal microscope, attacks in groups one immobilized *Alexandrium* cell then moves on to attack — still as a group — another cell without touching the other whole cells, suggesting active communication between *Vibrio* cells. *V. atlanticus* LGP32 (small cells); *A. pacificum* ACT03 (large cells).

Video 5. Vesicle formation and bursting of an *Alexandrium pacificum* ACT03. Direct effect of *Vibrio* supernatant on *Alexandrium* after 126 h of culture filmed under a confocal microscope